

Application of Surface wave methods for seismic site characterization

*Original*

Application of Surface wave methods for seismic site characterization / Foti, Sebastiano; Parolai, S.; Albarello, D.; Picozzi, M.. - In: SURVEYS IN GEOPHYSICS. - ISSN 0169-3298. - STAMPA. - 32:6(2011), pp. 777-825.  
[10.1007/s10712-011-9134-2]

*Availability:*

This version is available at: 11583/2440878 since:

*Publisher:*

Springer

*Published*

DOI:10.1007/s10712-011-9134-2

*Terms of use:*

This article is made available under terms and conditions as specified in the corresponding bibliographic description in the repository

*Publisher copyright*

(Article begins on next page)

# Application of Surface-wave methods for seismic site characterization

Sebastiano Foti<sup>1\*</sup>, Stefano Parolai<sup>2</sup>, Dario Albarello<sup>3</sup> and Matteo Picozzi<sup>2</sup>

<sup>1</sup> Politecnico di Torino, Italy

<sup>2</sup> Helmholtz Centre Potsdam GFZ German Research Centre for Geosciences, 14173 Potsdam Germany

<sup>3</sup> Università di Siena, Italy

\* corresponding author:

Dr. Sebastiano Foti

Assistant Professor

Dipartimento di Ingegneria Strutturale e Geotecnica,

Corso Duca degli Abruzzi, 24

Politecnico di Torino,

10129 - Torino – Italy

Fax: +39-011-564-4899

email: sebastiano.foti@polito.it

## ABSTRACT

Surface-wave dispersion analysis is widely used in geophysics to infer a shear wave velocity model of the subsoil for a wide variety of applications. A shear-wave velocity model is obtained from the solution of an inverse problem based on the surface wave dispersive propagation in vertically heterogeneous media. The analysis can be based either on active source measurements or on seismic noise recordings. This paper discusses the most typical choices for collection and interpretation of experimental data, providing a state of the art on the different steps involved in surface wave surveys. In particular, the different strategies for processing experimental data and to solve the inverse problem are presented, along with their advantages and disadvantages. Also, some issues related to the characteristics of passive surface wave data and their use in H/V spectral ratio technique are discussed as additional information to be used independently or in conjunction with dispersion analysis. Finally, some recommendations for the use of surface wave methods are presented, while also outlining future trends in the research of this topic.

## Keywords

Surface waves; inverse problems; seismic characterization; shear wave velocity; seismic noise; Rayleigh waves.

Post-print (i.e. final draft post-refereeing) version of an article published on SURVEYS IN GEOPHYSICS (ISSN 1084-0702), Volume 32, Issue. 6, pp. 777-825, November 2011.

Beyond the journal formatting, please note that there could be minor changes from this document to the final published version, accessible from <http://dx.doi.org/10.1007/s10712-011-9134-2>

The present version is accessible on PORTO, the Open Access Repository of Politecnico di Torino (<http://porto.polito.it>), in compliance with the Publisher's copyright policy as reported in the SHERPA-ROMEO website: <http://www.sherpa.ac.uk/romeo/issn/1084-0702/>

## 1. Introduction

Surface waves have been studied in seismology for the characterization of the Earth's interior since the 1920s, but their widespread use started during the 1950s and 1960s thanks to the increased possibilities of numerical analysis and to improvements in instrumentation for recording seismic events associated with earthquakes (Dziewonski and Hales, 1972; Aki and Richards, 1980; Ben-Menhaem and Sigh, 2000). Geophysical applications at regional scales for the characterization of geological basins make use of seismic signals from explosions (Malagnini et al., 1995) and microtremors (Horike, 1985). Engineering applications started in the 1950s with the Steady State Rayleigh Method (Jones, 1958), but their frequent use only began over the last two decades, initially with the introduction of the SASW (Spectral Analysis of Surface Waves) method (Stokoe et al., 1994) and then with the spreading of multistation methods (Park et al., 1999; Foti, 2000). The recent interest in surface waves methods in shallow geophysics is witnessed by numerous workshops and sessions at international conferences and by dedicated issues of international journals (EAGE – Near Surface Geophysics, November 2004; Journal of Engineering and Environmental Geophysics, June and September 2005). A comprehensive literature review on the topic is reported by Socco et al. (2010b).

Despite the different scales, the aforementioned applications rely on the same basic principles. They are founded on the geometrical dispersion, which makes the velocity of Rayleigh waves frequency dependent in vertically heterogeneous media. High frequency (short wavelength) Rayleigh waves propagate in shallow zones close to the free surface and are informative about their mechanical properties, whereas low frequency (long wavelength) components sample deeper layers. Surface wave methods use this property to characterize materials over a very wide range of scales, from microns to kilometres. The essential differences between applications are given by the frequency range of interest and the spatial sampling, as it will be detailed in next sections.

The basic principles of guided waves also find similar applications related to different waves. One example is electromagnetic waves generated by ground-penetrating radar (GPR) (Haney et al., 2010), which can be analysed to provide information on the water saturation of shallow sediments (Strobbia & Cassiani, 2007; van der Kruk et al., 2010).

Surface wave tests are typically devoted to the determination of a small strain stiffness profile for the site under investigation. Moreover, as shown by Malagnini et al. (1995) and Rix et al. (2000), surface wave data can also be used to characterize the dissipative behaviour of soils. Although this aspect will not be covered in detail in the present paper, it certainly deserves attention and further research considering the difficulties in getting reliable estimates of this using geophysical methods. Also, laboratory testing procedures on which damping estimates often rely upon are not representative of the behaviour of the whole soil deposit. Other relevant contributions to damping estimation from surface wave data are provided by Lai et al., 2002, Xia et al., 2002, Foti, 2004, Albarello and Baliva, 2009, and Badsar et al, 2010.

Another use of surface wave data is based on the analysis of seismic noise horizontal-to-vertical spectral ratios (NHV) in single station measurements of seismic noise. The ratio of the Horizontal-to-Vertical spectral components of seismic records was originally proposed as a tool for the determination of the resonance frequency of a soil deposit by Nogoshi and Igarashi (1970, 1971). Subsequently, the technique was revised by Nakamura (1989) and found large diffusion thanks to its cost effectiveness. The original interpretation of such information was based on the idea that peaks in the NHV were associated mainly with different amplifications of body wave propagating from the interior of the Earth. Nowadays, it is widely accepted that in most cases the peaks are associated with the surface wave content in the vertical and horizontal signals and as such they can be analysed to provide an estimate of the resonance frequencies of the layered system, which assumes the same values of the ones pertinent to the amplification of shear waves (Fäh et al., 2001; Malischewsky and Scherbaum, 2004). Inverse analysis can also be applied to the ellipticity of Rayleigh waves alone or

both Rayleigh and Love waves to provide information on the S-wave velocity below a site (Fäh et al., 2003), or in joint interpretation schemes with surface wave dispersion curves (Arai and Tokimatsu, 2005; Parolai et al., 2005).

The current paper is organised as follows: after a general overview on surface wave dispersion analysis, with the main focus on phase velocity, different experimental techniques either based on active-source or passive source measurements are discussed. Approaches and strategies proposed in the literature for the solution of the inverse problem are then covered. Finally some recommendations for the use and selection of surface wave methods for site characterization are reported.

## 2. Surface wave dispersion analyses

In order to summarize the concept behind the use of geometrical dispersion for soil characterization, let's assume that the stratified medium in Figure 1a is characterized by increasing stiffness, hence increasing shear-wave velocity, with depth. In such situation, a high frequency Rayleigh wave (i.e., a short wavelength, Figure 1b), travelling in the top layer will have a velocity of propagation slightly lower than the velocity of a shear wave in the first layer. On the other hand, a low frequency wave (i.e. a long wavelength, Figure 1c) will travel at a higher velocity because it is influenced also by the underlying stiffer materials. This concept can be extended to several frequency components. The phase velocity vs. wavelength (Figure 1d) plot will hence show an increasing trend for longer wavelengths. Considering the relationship between wavelength and frequency, this information can be represented as a phase velocity vs frequency plot (Figure 1e). This graph is usually termed a dispersion curve. This example shows, for a given vertically heterogeneous medium, that the dispersion curve will be associated with the variation of medium parameters with depth. This is the so called forward problem. It is important, however, to recognize the multimodal nature of surface waves in vertically heterogeneous media, i.e., several modes of propagation exist and higher modes can play a relevant role in several situations. Only the fundamental mode dispersion curve is presented in Figure 1.

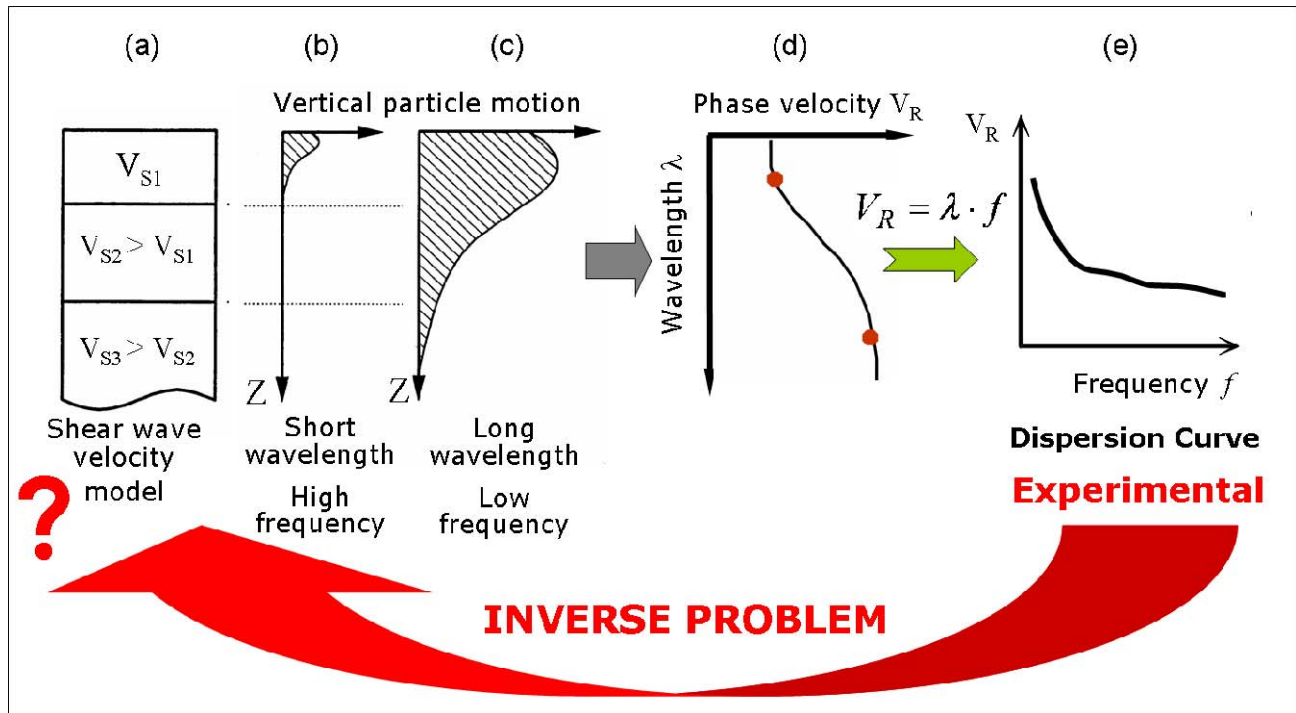


**Figure 1** – Parameter identification on the basis of geometrical dispersion

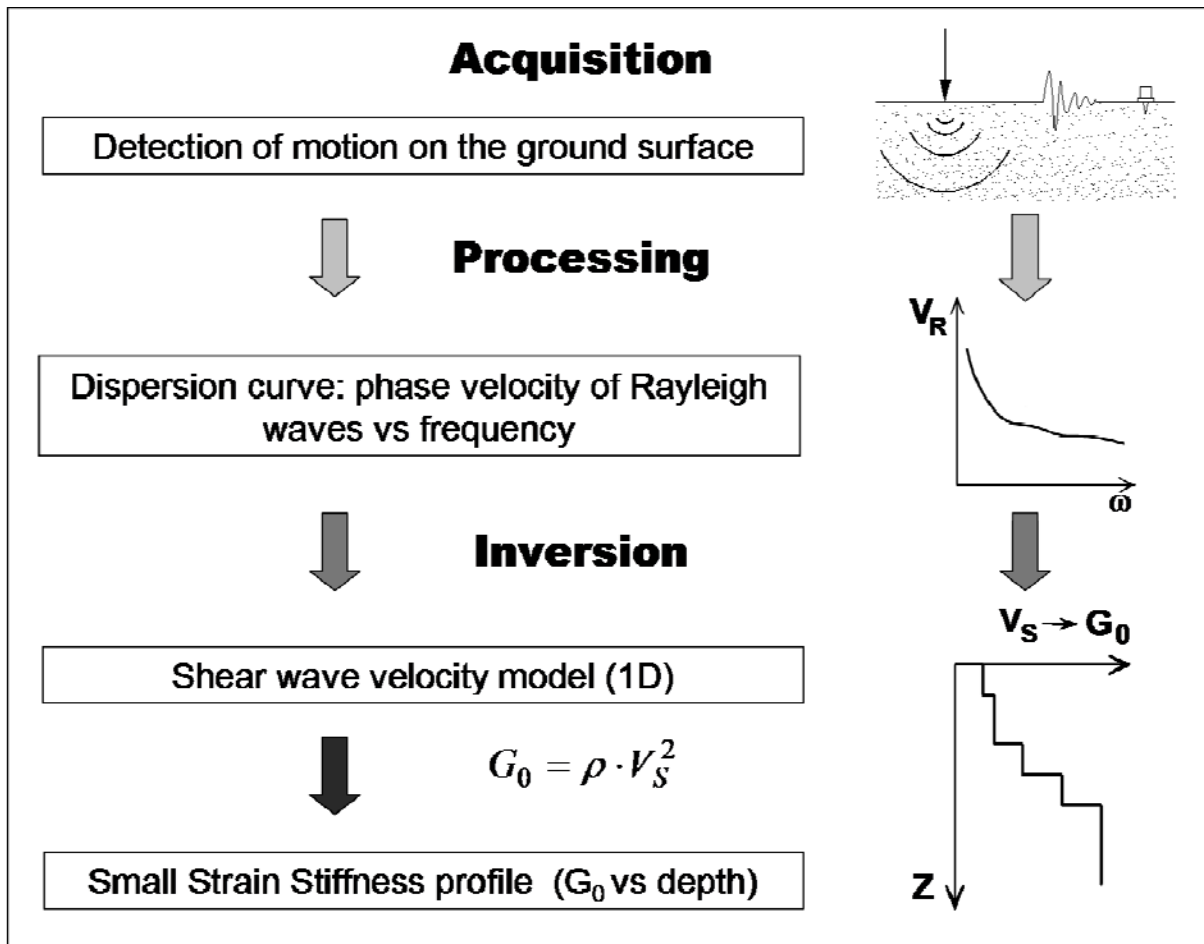
If the dispersion curve is estimated on the basis of experimental data, it is then possible to solve the inverse problem, i.e., the model parameters are identified on the basis of the experimental data collected on the boundary of the medium. This is the essence of surface wave methods.

Figure 2 outlines the standard procedure for surface wave tests, which can be subdivided into three main steps:

1. Acquisition of experimental data;
2. Signal processing to obtain the experimental dispersion curve;
3. An inversion process to estimate the shear wave velocity profile at the site.

It is very important to recognize that the above steps are strongly interconnected and their interaction must be adequately accounted for during the whole interpretation process.

Appealing alternatives for the interpretation of surface wave data are the inversion of field data based on full waveform simulations and the inversion of the Fourier frequency spectra of observed ground motion (Szelwis and Behle, 1987), but these strategies are rarely used because of their complexity. Moreover, the experimental dispersion curve is informative about trends to be expected in the final solution, so that its visual inspection is important for the qualitative validation of the results. Indeed, engineering judgment plays a certain role in test interpretation. Since the site and the acquisition are never “ideal”, the results of fully automated interpretation procedures must also be carefully examined, with special attention paid to intermediate results during each step of the interpretation process. A deep knowledge of the theoretical aspects and experience are hence essential.



**Figure 2** – Flow chart of surface wave tests.

Surface wave data can also be used to characterize the dissipative behaviour of soils. Indeed, the spatial attenuation of surface waves is associated with the internal dissipation of energy. Using a procedure analogous to the one outlined in Figure 2 it is possible to extract from field data the experimental attenuation curve, i.e., the coefficient of attenuation of surface waves as a function of frequency, and then use this information in an inversion process that aims to estimate the damping ratio profile for the site (Lai et al., 2002; Foti, 2004).

The primary use of surface wave testing is related to site characterization in terms of shear wave velocity profiles. The  $V_s$  profile is indeed of primary interest for seismic site response, vibration of foundations and vibration transmission in soils. Other applications are related to the prediction of ground settlement and to soil-structure interaction. Comparisons of results from surface wave tests and borehole tests are frequent in the technical and scientific literature, showing the reliability of the method (see, for example, Figure 3).

With respect to the evaluation of seismic site response, it is worth noting the affinity between the model used for the interpretation of surface wave tests and the model adopted for most site responses study. Indeed, the application of equivalent linear elastic methods is often associated with layered models, see for example the code SHAKE by Schnabel et al., 1972 s. This affinity is also particularly important in the light of equivalence problems, which arise because of the non-uniqueness of the solution in inverse problems. Indeed, profiles which are equivalent in terms of Rayleigh wave propagation are also equivalent in terms of seismic amplification (Foti et al., 2009).

Many seismic building codes (e.g., NEHRP, 2000; CEN, 2004) introduce the weighted average of the shear wave velocity profile in the shallowest 30m to discriminate classes of soil to which a similar site amplification effect can be associated. The so-called  $V_{s,30}$  can also be evaluated very efficiently with surface wave methods because its average nature does not require the high resolution provided by seismic borehole methods, such as Cross-Hole tests and Down-Hole tests (Moss, 2008; Comina et al., 2010).

A brief discussion of each step involved in surface wave testing is reported in the following section.

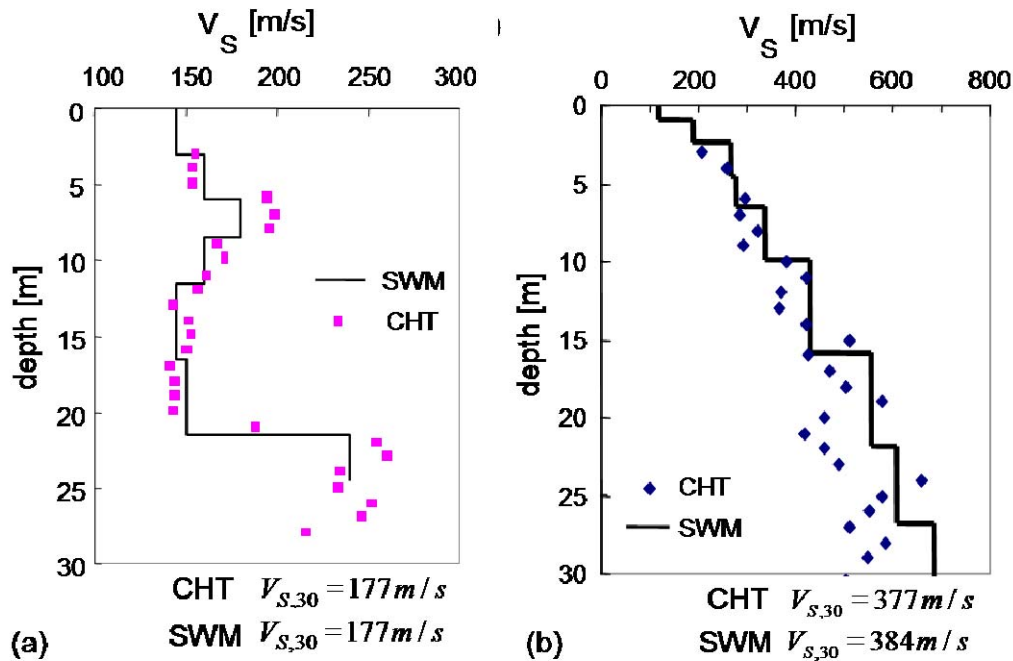


**Figure 3** – Comparisons between surface wave tests (SWM) and cross-hole tests (CHT) in terms of the associated shear wave velocity profiles and the equivalent  $V_{s,30}$  value: (a) Leaning Tower of Pisa site (data from Foti, 2003); (b) Saluggia site (data from Foti, 2000).

## 2.1. Acquisition

Surface wave data are typically collected on the surface using a variable number of receivers, which can be deployed both with one-dimensional (i.e., 1D) or two-dimensional (i.e., 2D) geometries. Several variations can be introduced both in the choice of receivers and acquisition device and in the generation of the wave fields.

The receivers adopted for testing related to exploration geophysics and engineering near surface applications are typically geophones (velocity transducers). Accelerometers are more often used for the characterization of pavement systems because in this case, the need for high frequency components makes the use of geophones not optimal.

The advantage of using geophones instead of accelerometers arises because geophones do not need a power supply, whereas accelerometers do. Moreover, in cases where surface waves are extracted from seismic noise recordings, accelerometers do not generally have the necessary sensitivity. On the other hand, low frequency geophones (natural frequency less than 2Hz) tend to be bulky and very vulnerable because the heavy suspended mass can be easily damaged during deployment on site.

Several devices can be used for the acquisition and storage of signals. Basically, any device having an A/D converter and the capability to store the digital data can be adopted, ranging from seismographs to dynamic signal analyzers to purpose-made acquisition systems built using acquisition boards connected to PCs or laptops. Commercial seismographs for geophysical prospecting are typically the first choice because they are designed to be used in the field, hence they are physically very robust. New generation seismographs are comprised of scalable acquisition blocks to be used in connection with field computers, hence allowing preliminary processing of data on site. As for as the generation of the wavefield is concerned, several different sources can be used, provided they generate sufficient energy in the frequency range of interest for the application. Impact sources are often preferred because they are quite low cost and allow for fast testing. A variety of impacts can be used ranging from small hammers for high frequency range signals (10-200 Hz), to large falling weights, which generate low frequency signals (2-40 Hz). Appealing alternatives are controlled sources which are able to generate a harmonic wave, hence assuring very high quality data. Also, the size of the source is variable from relatively small electromagnetic shakers to large truck-mounted vibroseis. The drawback of such sources is their cost and the need for longer acquisition processes on site. However, this aspect could be circumvented using swept-sine signals as input.

A different perspective is the use of seismic noise analysis. In this case the need for the source is avoided by recording background noise and the test is undertaken using a “passive” approach. Seismic noise consists of both cultural noise generated by human activities (traffic on highways, construction sites, etc.) and that associated with natural events (sea waves, wind, etc.). A great advantage is that seismic noise is usually rich in low frequency components, whereas high frequency components are strongly attenuated when they travel through the medium and are typically not detected. Hence, seismic noise surveys provide useful information for deep characterization (tens or hundreds of meters), whereas the level of detail close to the surface is typically low. In seismic noise surveys, however, the choice of the appropriate instrument is crucial (see e.g. Strollo et al., 2008 and references therein). Indeed, it is worth noting that due to the very low environmental seismic noise amplitude (i.e., the displacements involved are generally in the range  $10^{-4} - 10^{-2}$  mm), a prerequisite for high quality seismic noise recordings is the selection of A/D converters with adequate dynamic ranges (i.e., at least 19 bit).

The limitation in resolution close to the surface can be overcome by combining active and passive measurements, or with the new generation of low cost systems (Picozzi et al., 2010a) using a large number of sensors and high sampling rates.

## 2.2. Processing

The field data are processed to estimate the experimental dispersion curve, i.e., the relationship between phase velocity and frequency. The different procedures apply a variety of signal analysis tools, mainly based on the Fourier Transform. Indeed, using Fourier analysis, it is possible to separate the different frequency components of a signal that are subsequently used to estimate phase velocity using different approaches in relation to the testing configuration and the number of receivers. Alternative procedures are based on the group velocity of surface wave data, which can be obtained with the Multiple Filter Technique (Dziewonski et al., 1969) and its modifications (Levshin et al., 1992; Pedersen et al., 2003). These techniques do not suffer from spatial aliasing which affects estimates of phase velocity. However, here we will focus on phase velocity analysis, which is more widespread in the field of seismic site characterisation.

Some equipments allow for a pre-processing of experimental data directly in the field. Indeed the simple visual screening of time traces is not always sufficient because surface wave components are grouped together and without signal analysis it is not possible to judge the quality of data. In particular an assessment of the frequency range with high signal quality can be particularly useful to assess the necessity of changing the acquisition setup or the need for gathering additional experimental data. Ohrnberger et al. (2006) first proposed the use of wireless mobile ad-hoc network of standard seismological stations equipped with highly sensitivity, but also highly expensive, Earth Data digitizers for site-effect estimate applications. To overcome the resolution problem posed by a reduced number of stations available, the authors proposed to repeat the measurements using consecutive arrays with different sizes. Recently, Picozzi et al. (2010a) presented a new system, which is named GFZ-WISE, for performing dense 2D seismic ambient-noise array measurements. Since the system is made up of low-cost wireless sensing units that can form dense wireless mesh networks, raw data can be communicated to a user's external laptop which is connected to any node that belongs to the network, allowing a user to perform real-time quality control and analysis of seismic data.

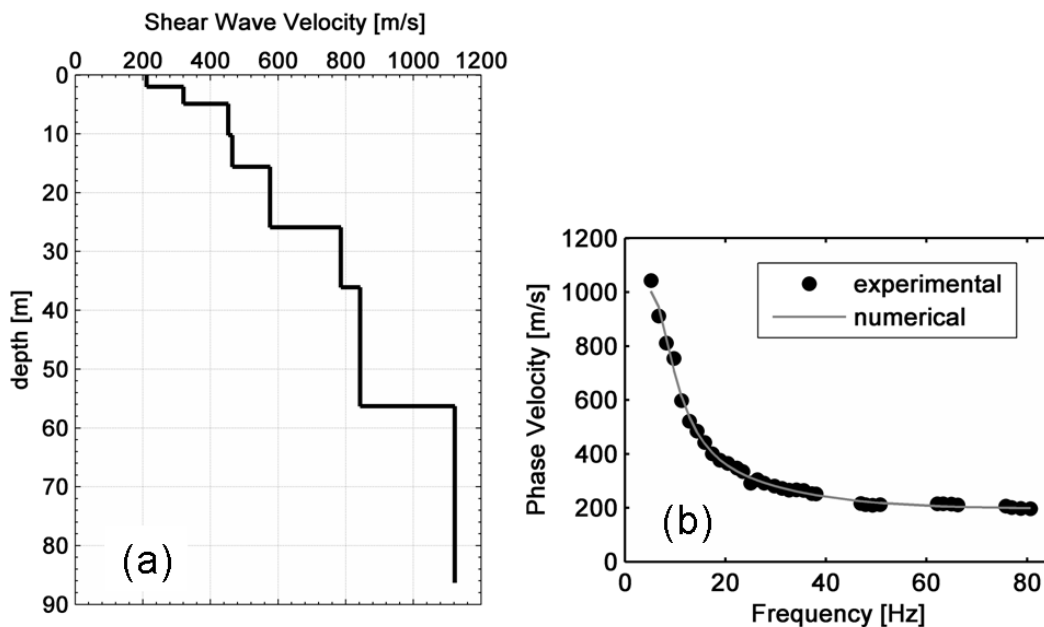


**Figure 4** – Example of the inversion process: (a) estimated shear wave velocity profile; (b) comparison between the correspondent numerical dispersion curve and the experimental one.



### 2.3. Inversion

The solution of the non linear inverse problem is the final step in the test interpretation. Assuming a model for the soil deposit, model parameters that minimize an object function representing the distance between the experimental and the numerical dispersion curves are identified. The object function can be expressed in terms of any mathematical norm (usually the RMS) of the difference between experimental and numerical data points. In practice, the set of model parameters that produces a solution of the forward problem (a numerical dispersion curve) as close as possible to the experimental data (the experimental dispersion curve of the site) is selected as the solution of the inverse problem (e.g., Figure 4).

This goal can be reached using a variety of strategies. A major distinction arises between Local Search Methods (LSM), which minimize the difference starting from a tentative profile and searching in its vicinity, and Global Search Methods (GSM), which attempt to explore the entire parameter space of possible solutions. As can also be intuitively imagined, both methods present advantages and drawbacks.

LSMs are undoubtedly faster since they require a limited number of runs of the forward Rayleigh wave propagation problem, but since the solution is searched in the vicinity of a tentative profile, there is the risk of being trapped in local minima. On the other hand, LSMs allow the estimation of the resolution and model covariance matrixes, which are powerful tools for verifying the existence of trade-off among model parameters, and for assessing the confidence bounds for the unknown parameters.

On the other side GSMs require a much bigger computational effort since a large number of forward calculations is required, so that the approach is quite time consuming. However, GSMs are considered inherently stable methods, because they require the computation of the forward problem and of the cost function only, avoiding any potentially numerically instable process (e.g., matrix inversion and partial derivative estimates).

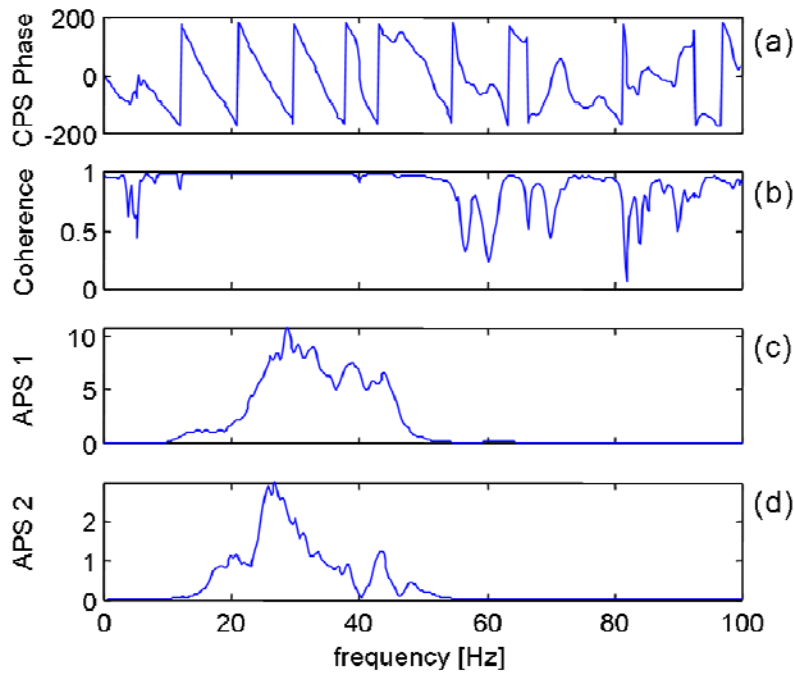


**Figure 5** – Example of a two-receiver data elaboration (source: 130kg weight-drop, inter-receiver distance 18m): a) cross power spectrum (wrapped); b) coherence function; c) Auto-power spectrum (receiver 1); d) Auto-power spectrum (receiver 2) (Foti, 2000).

In general, surface wave dispersion curve inverse problems are inherently ill-posed and a unique solution does not exist. A major consequence is the so called equivalence problem, i.e., several shear wave velocity profiles can be equivalent with respect to the experimental dispersion curve, meaning that the numerical dispersion curve associated to each of these profiles are at the same distance from the experimental dispersion curve. A meaningful evaluation of equivalent profiles has also to take into account the uncertainties in the experimental data. Additional constraints and a priori information from borehole logs or other geophysical tests are useful elements in resolving the equivalence problem.

### 3. Active source methods

#### 3.1. Spectral Analysis of Surface Waves (SASW)

The traditional SASW method uses either impulsive sources such as hammers or steady-state sources like vertically oscillating hydraulic or electro-mechanical vibrators that sweep through a pre-selected range of frequencies, typically between 5 and 200 Hz. Rayleigh waves are detected by a pair of transducers located at distances  $D$  and  $D+X$  from the source. The signals at the receivers are digitised and recorded by a dynamic signal analyser. The Fast Fourier Transform is computed for each signal and the cross power spectrum between the two receivers is calculated. Multiple signals are averaged to improve the estimate of the cross power spectrum. An impact source creates a wave-train, which has components over a broad frequency range. The ground motion is detected by a pair of receivers, which are placed along a straight line passing from the source, and the signals are then analysed in the frequency domain. The phase velocity  $V_R$  is obtained from the phase difference of the signals using the following relationship:

$$V_R(\omega) = \frac{\omega}{\Theta_{12}(\omega)} \cdot X \quad (1)$$

in which  $\Theta_{12}(\omega)$  is the cross-power spectrum phase between two receivers,  $\omega$  is the angular frequency and  $X$  is the inter-receiver spacing.

One critical aspect of the above procedure is the influence of the signal-to-noise ratio. Indeed, the measurement of phase difference is a very delicate task. The necessary check on the signal-to-noise ratio is usually accomplished using the coherence function (Santamarina and Fratta, 1998), whose value is equal to 1 for linearly correlated signals in the absence of noise. Only the frequency ranges having a high value of the coherence function are used for the construction of the experimental dispersion curve. It must be remarked that the coherence function must be evaluated using several pairs of signals, leading to the necessity of repeating the test using the same receiver setup.

As an example, Figure 5 shows the spectral quantities relative to a pair of receivers the couple with 18m spacing, selected from a test performed using a weight-drop source. Together with the Cross-Power Spectrum phase, the Coherence function and the Auto-Power spectra at the two receivers are reported. These other quantities give a clear picture of the frequency range over which most of the energy is concentrated and hence there is a high signal-to-noise ratio.

Other important concerns are near-field effects and spatial aliasing in the recorded signals. In this respect, usually a filtering criterion (function of the testing setup) is applied to the dispersion data (Ganji et al., 1998), e.g., only frequencies for which the following relationship is satisfied are retained:

$$\frac{X}{3} < \lambda_R(\omega) < 2D \quad (2)$$

where  $\lambda_R(\omega) = V_R(\omega)/f$  is the estimated wavelength,  $D$  is the source-first geophone distance, and  $X$  is the inter-receiver spacing (Fig. 6). Typically, the receiver positions are such that  $X$  and  $D$  are equal, in accordance with the results of some parametric studies about the optimal test configuration (Sanchez-Salintero, 1987).

The above filtering criterion assumes that near-field effects are negligible if the first receiver is placed at least half a wavelength away from the source for a given frequency in the spectral analysis. Such an assumption is acceptable in a normally dispersive site, i.e., a site having stiffness increasing with depth, but it can be too optimistic for more complex situations (Tokimatsu, 1995). For this reason and in order to avoid a significant loss of data, inversion methods that take into account near field effects have been proposed (Roesset et al., 1991, Ganji et al., 1998).

For the aforementioned considerations, a single testing configuration gives information only for a particular frequency range, which is dependent on the receiver positions. The test is then repeated using a variety of geometrical configurations that include adapting the source type to the actual configuration, i.e., lighter sources (hammers) are used for high frequencies (small receiver spacing) and heavier ones (weight-drop systems) for low frequencies (large receiver spacing). Usually five or six setups are used, moving source and receivers according to a common-receiver-midpoint scheme (Nazarian and Stokoe, 1984).

Typically, the test is repeated for each testing configuration in a forward and reverse direction, moving the source from one side to the other with respect to the receivers (Figure 6a). Such a procedure is quite time consuming, but it is required to avoid the drift that can be caused by instrument phase shifts between the receivers, since the analysis process is based on a delicate phase difference measurement. Yet, very often the measurements are conducted using a common source scheme (Figure 6b) in order to avoid the need for moving the source, especially when it cannot be easily moved (i.e. large and heavy sources).

Finally, the information collected in several testing configurations is assembled (Figure 7) and averaged to estimate the experimental dispersion curve at the site, which will be used for the subsequent inversion process.

A crucial task in the interpretation of the SASW test is related to the unwrapping of the Cross-Power Spectrum phase. This is obtained in a modulo- $2\pi$ , which is very difficult to interpret and unsuitable for further processing (Poggiagliolmi et al., 1982). The passage to an unwrapped (full-phase) curve is necessary for the computation of time delay as a function of frequency (see Equation 1).

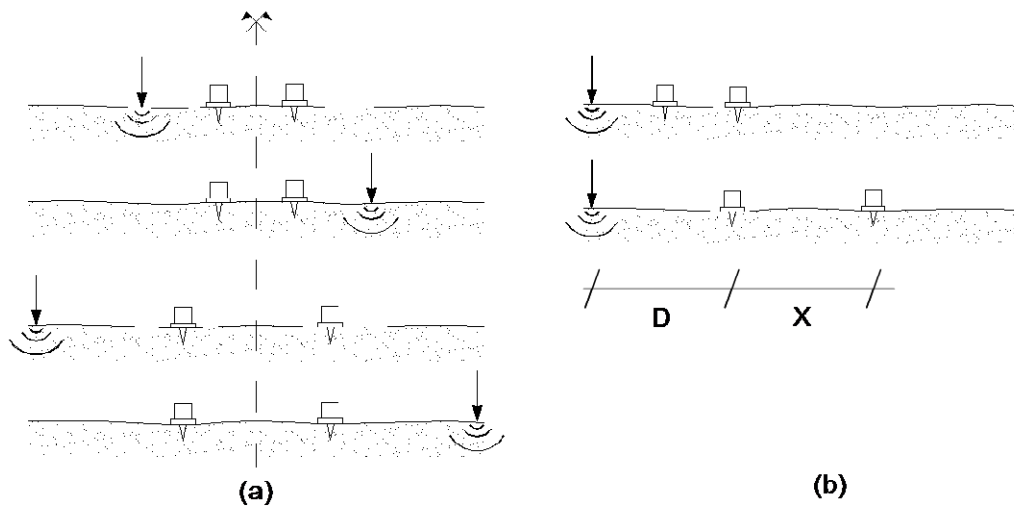


**Figure 6** – Acquisition schemes for 2-station SASW: a) common receiver mid-point; b) common source (Foti, 2000)

Usually, some automated algorithms are applied for this task (Poggiagliolmi et al., 1982), but external noise can produce fictitious jumps in the wrapped phase, which drastically damage the results. The operator may not always be able to correct such unwrapping errors on the basis of judgement and in any case, it is a subjective procedure, which precludes the automation of the process. The unwrapping procedure begins in the low frequency range where there is a very low signal-to-noise ratio, but error in the unwrapping of low frequencies might also affect velocity estimation also in the frequency range where the signal-to-noise ratio is good. An automated procedure based on a least-square interpolation of the cross-power spectrum phase has also been proposed (Nazarian and Desai, 1993).

### 3.2. Multi-channel Analysis of Surface Waves (MASW)

The use of a multi-station testing setup can introduce several advantages in surface wave testing. In this case, the motion generated by the source is detected simultaneously at several receiver locations in line with the source itself. This testing setup is similar to the one used for seismic refraction/reflection surveys, providing interesting synergies between different methods (Foti et al., 2003; Ivanov, 2006; Socco et al., 2010a).

For surface wave analysis, the experimental data are typically transformed from the time-offset domain to different domains, where the dispersion curve is easily extracted from the spectral maxima. For example, applying a double Fourier transform to field data the dispersion curve can be identified as the maxima in the frequency-wavenumber domain (Figure 8). Other methods use different transforms obtaining similar results, e.g., the  $\omega$ - $p$  (frequency-slowness) domain representation obtained by the slant-slack transform (McMechan & Yedlin, 1981) or the MASW method (Park et al., 1999). The formal equivalence of these approaches can be proved considering the mathematical properties of the different transforms (Santamarina & Fratta, 1998) and there is practically no difference in the obtained dispersion curves (Foti, 2000). An alternative method for extracting the surface wave dispersion curve from multistation data is based on the linear regression of phase versus offset at each frequency (Strobbia and Foti, 2006).

In theory, transform-based methods allow the identification of several distinct Rayleigh modes. Tselentis and Delis (1998) showed that the  $f$ - $k$  spectrum for surface waves in layered media can be written as the following sum of modal contributions:

$$F(f, k) = \sum_m S_m(f) \cdot \left[ \sum_{n=1}^N e^{-\alpha_m(f) \cdot x_n} \cdot e^{i(k - k_m(f)) \cdot x_n} \right] \quad (3)$$

where  $S_m$  is a source function,  $x_n$  is the distance from the source of the  $n^{\text{th}}$  receiver,  $\alpha_m$  and  $k_m$  are respectively attenuation and wavenumber for the  $m^{\text{th}}$  mode. Note that the above expression is valid in the far field (Aki and Richards, 1980) and that the geometrical spreading is neglected because it can be accounted for in processing (Tselentis and Delis, 1998). Observing the quantity in the square brackets in eq. 3, it is evident that, if material attenuation is neglected, the maxima of the energy spectrum are obtained for  $k = k_m(f)$ . Furthermore, it can be shown that also if the above differentiation is conducted without neglecting the material attenuation, the conclusion is the same, i.e., the accuracy is not conditioned by material attenuation (Tselentis and Delis 1998).

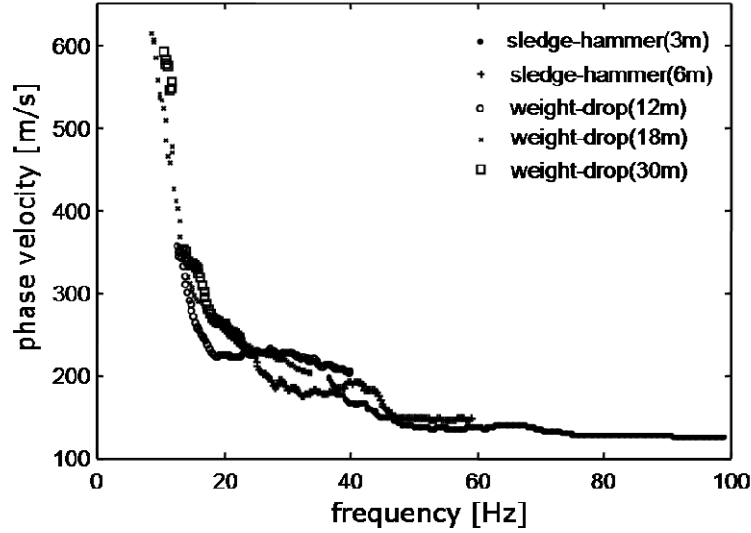


**Figure 7** – Assembling dispersion curves branches in SASW method (Foti, 2000)

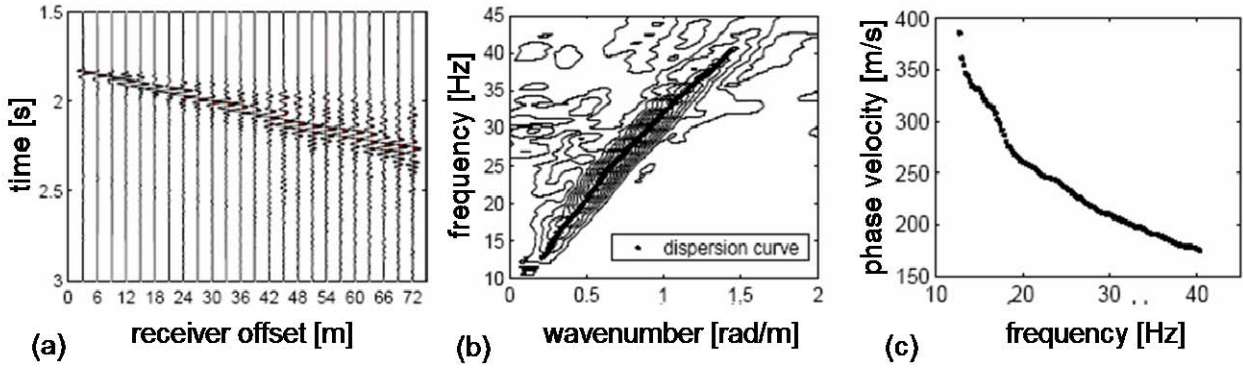


**Figure 8** – Example of processing of experimental data using the frequency-wavenumber analysis: (a) field data; (b)  $f-k$  domain ; (c) dispersion curve (Foti, 2005)

Once the modal wavenumbers have been estimated for each frequency, they can be used to evaluate the dispersion curve, recalling that phase velocity is given by the ratio between frequency and wavenumber.

Using a very large number of signals (256) Gabriels et al. (1987) were able to identify six experimental Rayleigh modes for a site. They then used these modes for the inversion process. The possibility of using modal dispersion curves is a great advantage with respect to methods giving only a single dispersion curve (as the two-station method) because having more information means a better constrained inversion. Nevertheless it has to be considered that in standard practice, the number of receivers for engineering applications is typically small and the resulting reduced spatial sampling strongly affects the resolution of the surface wave test. Receiver spacing influences aliasing in the wavenumber domain, so that if high frequency components are to be sought, the spacing must be small. On the other side, the total length of the receiver array influences the resolution in the wavenumber domain. Obviously, using a finite number of receivers this aspect generates a trade-off similar to the one existing between resolution in time and in frequency, as the resolution in the wavenumber domain is inversely proportional to the total length of the acquisition array. Using a simple 2D Fourier Transform on the original dataset to obtain the experimental  $f-k$  domain would lead to a spatial resolution not sufficient to obtain a reliable estimate of the dispersion curve. The use of zero padding or advanced spectral analysis techniques such as beamforming or

MUSIC (Zwicky, 1999) makes it possible to locate the correct position of the maxima in the  $fk$  panel (Figure 9).

Unfortunately, once a survey has been carried out adopting a certain array configuration, no signal analysis strategies can allow the improvement of the real resolution. Hence, in the following signal analysis stage, it will not be possible anymore to separate modal contributions when more than a single mode plays a relevant role in the propagation (Foti et al., 2000). This aspect is exemplified in Figure 10 where slices of the  $fk$  spectrum for a given frequency are reported for two different synthetic datasets. If a large number of receivers is used to estimate the  $fk$  spectrum, the resolution is very high and the energy peaks are well defined, but if the number of receivers is low, the resolution is very poor. With poor resolution it is only possible to locate a single peak in the  $fk$  panel, which in principle is not associated with a single mode but to several superposed modes. The concept of apparent phase velocity has been introduced to denote the velocity of propagation corresponding to this single peak representing several modes (Tokimatsu, 1995). In the example of Figure 10a, the fundamental mode is the dominant mode in the propagation, meaning that almost all energy is associated with this mode. In this situation, the apparent phase velocity is the phase velocity associated with the fundamental mode and the inversion process can be simplified inverting the apparent dispersion curve as a fundamental mode. This situation is usual in soil deposits where stiffness increases with depth with no marked impedance jumps between different layers. On the contrary, in the example of Figure 10b, the fundamental mode is still the one carrying more energy, but it is no longer dominant, meaning that higher modes play a relevant role in the propagation. If few receivers are used, a single peak will be observed and a single value of the phase velocity will be obtained. This value is not necessarily the phase velocity of one of the modes involved in the propagation, but it is rather a sort of average value, often referred to as the apparent phase velocity or effective phase velocity (Tokimatsu, 1995). In this case, it is no longer possible to use inversion processes based on the fundamental mode or on modal dispersion, but it is necessary to use an algorithm that can account for mode superposition effects (Lai, 1998) and for the actual testing configuration (O'Neill, 2004). This situation is usual when strong impedance contrasts are present in the soil profile or in inversely dispersive profiles, i.e., profiles in which soft layers underlie stiff layers.

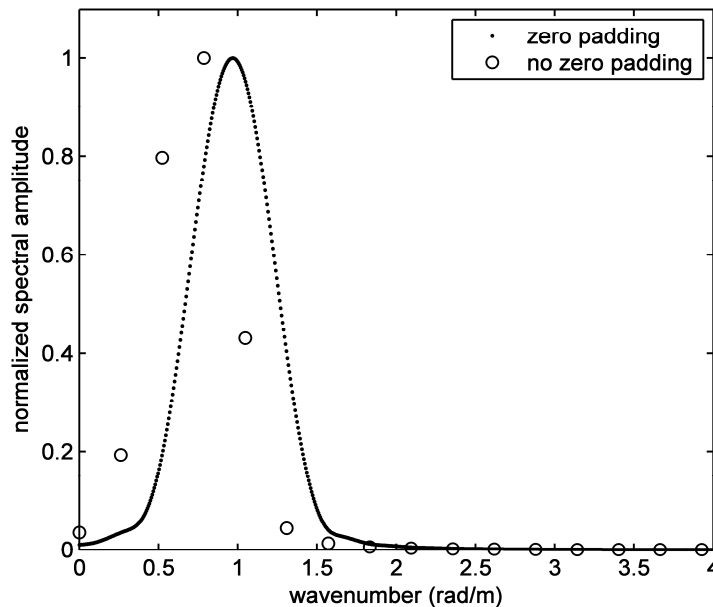


**Figure 9** – Effect of zero padding on resolution in the wavenumber domain: slice of the  $fk$  panel for a given frequency (Foti, 2005).

The dispersion curves obtained with  $fk$  analysis on the synthetic dataset used for Figure 10b are reported in Figure 11. As explained above, if a sufficiently high number of receivers is used, it will be possible to obtain the modal dispersion curves (Figure 11a), whereas with the number of receivers used in standard practice, a single apparent dispersion curve will be obtained (Figure 11b).

As mentioned above, the apparent dispersion curve is dependent on the spatial array so that if higher modes are relevant for a given site, the inversion process will be cumbersome. On the other hand, if the fundamental mode is dominant, the inversion process can be noticeably simplified. However, it is not always clear from the simple inspection of the experimental dispersion curve if higher modes are involved.

#### 4. Passive source methods

##### 4.1. Refractor Microtremor (ReMi)

Similarly to the MASW method, the multi-station approach can be applied to seismic noise recordings collected by 1D arrays. This technique, generally known as Refraction Microtremors (ReMi) was recently introduced by Louie (2001) who proposed as a basis for the velocity spectral analysis the  $p$ - $\tau$  transformation, or “slantstack”, described by Thorson and Claerbout (1985). This transformation takes a record section of multiple seismograms, with seismogram amplitudes relative to distance and time ( $x$ - $t$ ), and converts them to amplitudes relative to the ray parameter  $p$  (the inverse of apparent velocity) and an intercept time  $\tau$ . It is familiar to array analysts as “beam forming”, and has similar objectives as the two-dimensional Fourier-spectrum or “ $f$ - $k$ ” analysis as described by Horike (1985).

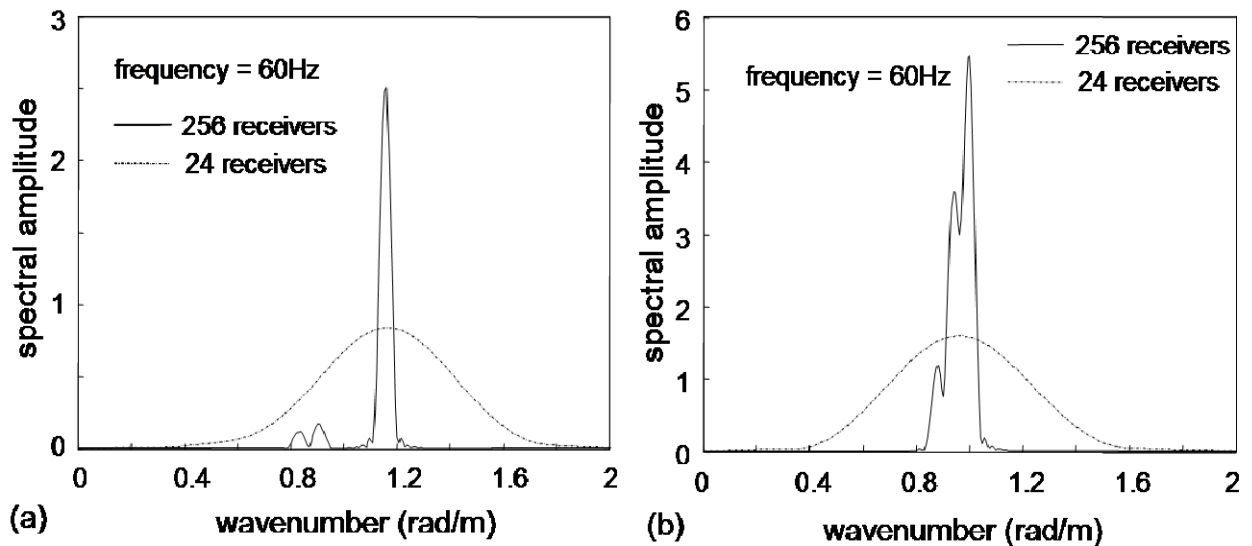


**Figure 10** – Influence of the effective wavenumber resolution on the dispersion curve (a) dominant fundamental mode (b) relevant higher modes (Foti, 2005)

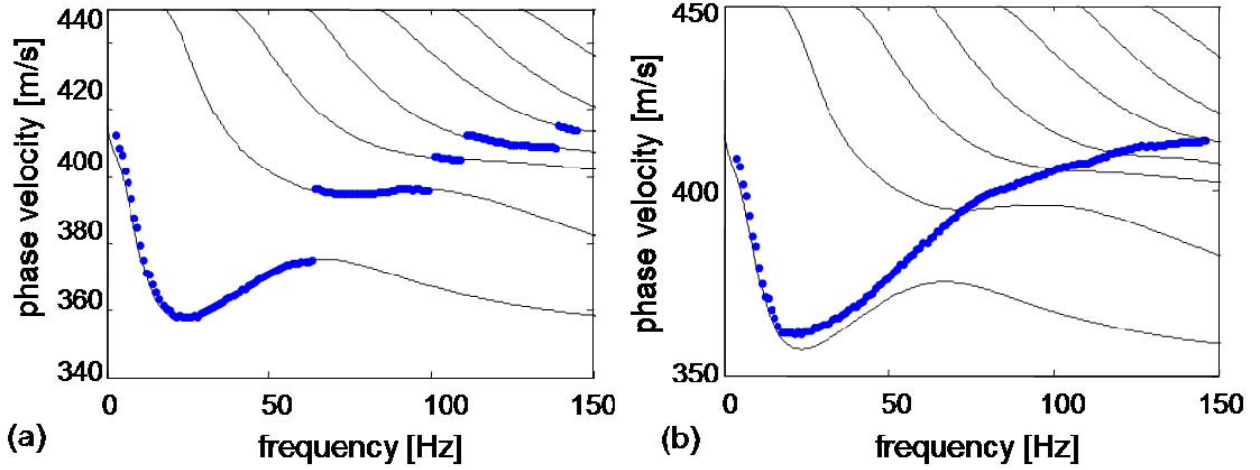


**Figure 11** – Influence of wavenumber resolution on the dispersion curve from synthetic data: (a) 256 receivers; (b) 24 receivers (Foti, 2000)

The  $p$ - $\tau$  transform is a simple line integral across a seismic record  $A(x, t)$  in distance  $x$  and time  $t$ :

$$A(p, \tau) = \int_x A(x, t = \tau + p x) dx \quad (4)$$

where the slope of the line  $p = dt/dx$  is the inverse of the apparent velocity  $V_a$  in the  $x$  direction. In practice,  $x$  is discretized into  $nx$  intervals at a finite spacing  $dx$ . That is  $x = j dx$  where  $j$  is an integer. Likewise, time is discretized with  $t = i dt$  (with  $dt$  usually 0.001-0.01 second), giving a discrete form of the  $p$ - $\tau$  transform for negative and positive  $p = p0 + l dp$ , and  $\tau = k dt$  is called the slantstack:

$$A(p = p0 + l dp, \tau = k dt) = \sum_{j=0, nx-l} A(x = j dx, t = i dt = \tau + p x) \quad (5)$$

The calculation starts from an initial  $p0 = -p_{max}$  where  $p_{max}$  defines the inverse of the minimum velocity that will be tested.  $np$  is set to vary between one and two times  $nx$ .  $dp$  typically ranges from 0.0001-0.0005 sec/m, and is set to cover the interval from  $-p_{max}$  to  $p_{max}$  in  $2np$  slowness steps. In this way, energy propagating in both directions along the refraction receiver line will be considered. Amplitudes at times  $t = \tau + p x$  falling between sampled time points are estimated by linear interpolation.

The distances used in ReMi analysis are simply the distances between geophones starting from one end of the array. As described by Thorson and Claerbout (1985), the traces do not have to sample the range of distance. The intercept times after transformation are thus simply the arrival times at one end of the array.

Each trace in the  $p$ - $\tau$  transformed record contains the linear sum across a record at all intercept times, at a single slowness or velocity value. The next step takes each  $p$ - $\tau$  trace in  $A(p, \tau)$  (eq. 5) and computes its complex Fourier transform  $F_A(p, f)$  in the  $\tau$  or intercept time direction and its power spectrum  $S_A(p, f)$ .

Then, the two  $p$ - $\tau$  transforms of a record obtained by considering the forward and reverse directions of propagation along the receiver line are summed together. To sum energy from the forward and reverse directions into one slowness axis that represents the absolute value of  $p$ ,  $|p|$ , the slowness axis is folded and summed about  $p=0$ .

This operation completes the transform of a record from distance-time ( $x$ - $t$ ) into the  $p$ -frequency ( $p$ - $f$ ) space. The ray parameter  $p$  for these records is the horizontal component of slowness (inverse velocity) along the array. In analyzing more than one record from a ReMi deployment the individual records'  $p$ - $f$  images are added point-by-point into an image of summed power.



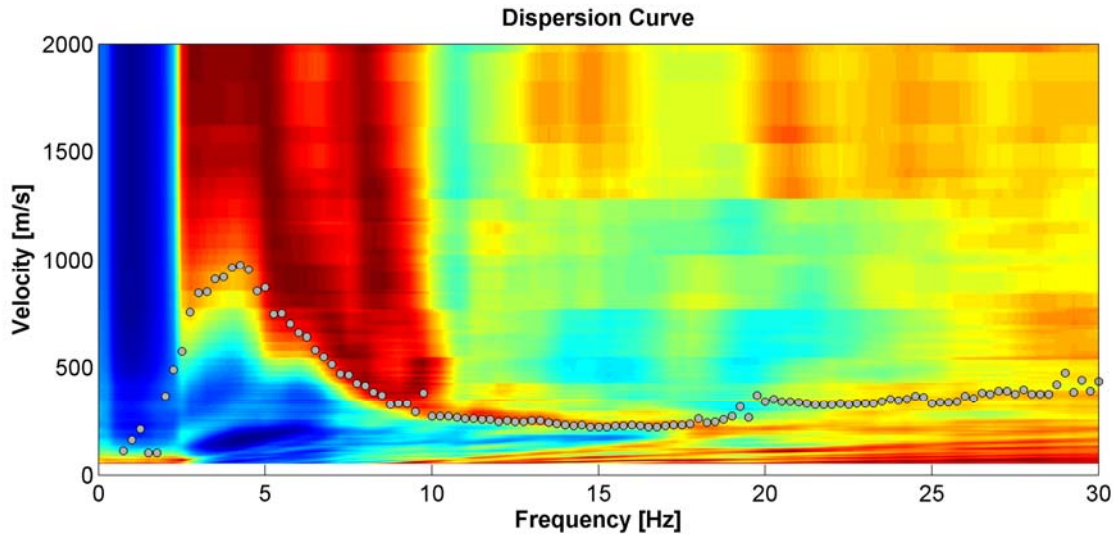


**Figure 12** – ReMi and ESAC analysis results comparison. ESAC phase velocities (gray dots).

Therefore, the slowness-frequency analysis produces a record of the total spectral power considering all records from a site, which plots within slowness-frequency ( $p$ - $f$ ) axes. If one identifies trends within this domain where a coherent phase has significant power, then the slowness-frequency picks can be plotted on a typical frequency-velocity diagram for dispersion analysis. The  $p$ - $\tau$  transform is linear and invertible, and can in fact be completed equivalently in the spatial and temporal frequency domains (Thorson and Claerbout, 1985). Following Louie (2001), due to the use of linear geophone arrays and to the fact that the location of environmental seismic noise sources cannot be estimated, an interpreter cannot just pick the phase velocity of the largest spectral ratio at each frequency as a dispersion curve, as MASW analyses effectively do. On the contrary, an interpreter must try to pick the lower edge of the lowest-velocity, but still reasonable peak ratio. Since the arrays are linear and do not record an on-line triggered source, some noise energy will arrive obliquely and appear on the slowness-frequency images as peaks at apparent velocities  $V_a$  higher than the real in-line phase velocity  $v$ . In the presence of an isotropic or weakly heterogeneous wave field, it can be demonstrated (Louie, 2001; Mulargia and Castellaro, 2008) that out-of-line wave fronts do not affect significantly the Rayleigh waves dispersion curve. However, this is not true when markedly directional effects exist. In this respect, 2D arrays (see next section) provide the capability to resolve obliquely incident energy. An example of the application of the ReMi technique can be found in Stephenson et al. (2005) and Richwalski et al. (2007).

Interestingly, Figure 12 shows that starting from the same 1D recording data-set, the dispersion curve obtained using the ESAC signal analysis (see the following section for details on the ESAC analysis) automatically corresponds to the lower edge of the maxima energy distribution within the ReMi's frequency-velocity plot. It is worth noting that the combination of the ReMi and ESAC analyses would allow thus eliminating the questionable and unclear, especially for un-experienced interpreters, manual velocity picking analysis step introduced in Louie (2001).

#### 4.2. Two-dimensional (2D) arrays

Seismic arrays were originally proposed at the beginning of the 1960s as a new type of seismological tool for the detection and identification of nuclear explosion (Frosch and Green, 1966). Since then, seismic arrays have been applied at various scales for many geophysical purposes. At the seismological scale, they were used to obtain refined velocity models of the Earth's interior (e.g., Birtill and Whiteway, 1965; Whiteway, 1966; Kväerna, 1989; Kárasón and van der Hilst, 2001; Ritter et al., 2001; Krüger et al., 2001). A recent review on array applications in seismology can be found in Douglas (2002) and in Rost and Thomas (2002). At smaller scales, since

the pioneering work of Aki (1957), seismic arrays have been used for the characterization of surface wave propagation, and the extraction of information about the shallow subsoil structure (i.e., the estimation of the local S-wave velocity profile). Especially in the last decades, due to the focus of seismologists and engineers on estimating the amplification of earthquake ground motion as a function of local geology, and the improvements in the quality and computing power of instrumentation, interest in analyzing seismic noise recorded by arrays (e.g., among others Horike, 1985; Hough et al., 1992; Ohori et al., 2002; Okada, 2003; Scherbaum et al. 2003, Parolai et al., 2005) has grown.

#### 4.2.1. frequency-wavenumber (f-k) based methods

The phase velocity of surface waves can be extracted from noise recordings obtained by 2D seismic arrays by using different methods, originally developed for monitoring nuclear explosions. Here we will illustrate the two most frequently used methods for  $f$ - $k$  analysis: the Beam-Forming Method (BFM) (Lacoss et al., 1969) and the Maximum Likelihood Method (MLM) (Capon, 1969).

The estimate of the  $f$ - $k$  spectra  $P_b(f,k)$  by the BFM is given by:

$$P_b(f, k) = \sum_{l,m=1}^n \phi_{lm} \exp\{ik(X_l - X_m)\} , \quad (6)$$

where  $f$  is the frequency,  $k$  the two-dimensional horizontal wavenumber vector,  $n$  the number of sensors,  $\phi_{lm}$  the estimate of the cross-power spectra between the  $l^{\text{th}}$  and the  $m^{\text{th}}$  data, and  $X_l$  and  $X_m$ , are the coordinates of the  $l^{\text{th}}$  and  $m^{\text{th}}$  sensors, respectively.

The MLM gives the estimate of the  $f$ - $k$  spectra  $P_m(f,k)$  as:

$$P_m(f, k) = \left( \sum_{l,m=1}^n \phi_{lm}^{-1} \exp\{ik(X_l - X_m)\} \right)^{-1} . \quad (7)$$

Capon (1969) showed that the resolving power of the MLM is higher than that of the BFM, however, the MLM is more sensitive to measurement errors.

From the peak in the  $f$ - $k$  spectrum occurring at coordinates  $k_{xo}$  and  $k_{yo}$  for a certain frequency  $f_0$ , the phase velocity  $c_0$  can be calculated by:

$$c_0 = \frac{2\pi f_0}{\sqrt{k_{xo}^2 + k_{yo}^2}} . \quad (8)$$

An extensive description of these methods can be found in Horike (1985) and Okada (2003).

As discussed in section 2.2 about the MASW method, the  $f$ - $k$  analyses presented here can be also applied to recordings collected using 1D geometry.

The estimate  $EP_b$  and  $EP_m$  of the true  $P_b$  and  $P_m$   $f$ - $k$  spectra may be considered the convolution of the true functions with a frequency window function  $W_f$  and the wavenumber window functions  $W_B$  and  $W_M$  for the BFM and MLM, respectively (Lacoss *et al.*, 1969). The first window function  $W_f$  is the transfer function of the tapering function applied to the signal time windows (Kind et al., 2005). The function  $W_B$ , is referred to differently by various authors (e.g., “*spatial window function*” by Lacoss et al., 1969, and “*beam-forming array response function*” by Capon, 1969), and hereafter is termed the Array Response Function (ARF). The ARF depends only on the distribution of stations in the array, and for the wavenumber vector  $k_o$  has the form (Horike, 1985)

$$W_B(k, k_o) = \frac{1}{n^2} \sum_{l,m=1}^n \exp\{i(k - k_o)(X_l - X_m)\} \quad (9)$$

Simply speaking, it represents a kind of spatial filter for the wavefield. The main advantage of the MLM with respect to the BFM involves the use of an improved wavenumber window  $W_M$ . That is, for a wavenumber  $k_0$ , this window function may be expressed in the form

$$W_M(f, k, k_0) = \left| \sum_{j=1}^N A_j(f, k_0) \right| W_B(k, k_0) \quad (10)$$

Where

$$A_j(f, k_0) = \frac{\sum_{l=1}^N q_{jl}(f, k_0)}{\sum_{j,l=1}^N q_{jl}(f, k_0)} \quad (11)$$

and  $q_{jl}$  represents the elements of the cross-power spectral matrix. It is evident that  $W_M$  depends not only on the array configuration through the function  $W_B$ , but also on the quality (i.e., signal-to-noise ratio) of the data (Horike, 1985). In fact, the wavenumber response is modified by using the weights  $A_j(f, k_0)$ , which depend directly on the elements  $q_{jl}(f)$ . In practice,  $W_M$  allows the monochromatic plane wave travelling at a velocity corresponding to the wavenumber  $k_0$  to pass undistorted, while it suppresses, in an optimum least-square sense, the power of those waves travelling with velocities corresponding to wavenumbers other than  $k_0$  (Capon, 1969). Or, in other words, coherent signals are associated with large weights of  $A_j$  and their energy is emphasized in the  $f$ - $k$  spectrum. On the contrary, if the coherency is low, the weights  $A_j$  are small and the energy in the  $f$ - $k$  spectrum is damped (Kind et al., 2005). This automatic change of the main-lobe and side-lobe structure for minimizing the leakage of power from the remote portion of the spectrum has a direct positive effect on the  $P_m$  function, and consequently on the following velocity analysis. However, considering the dependence of  $W_M$  on  $W_B$ , it is clear that the array geometry is a factor having a strong influence on both  $EP_b$  and  $EP_m$ . In fact, similarly to every kind of filter, several large side lobes located around the major central peak can remain in the  $f$ - $k$  spectra (Okada, 2003) and determine serious biases in the velocity and back-azimuth estimates. In particular, the side-lobe height and main-lobe width within  $W_B$  control the leakage of energy and resolution, respectively (Zywicki, 1999).

As a general criterion, the error in the velocity analysis due to the presence of spurious peaks in the  $f$ - $k$  spectra may be reduced using distributions of sensors for which the array response approaches a two-dimensional  $\delta$ -function. For that reason, it is considered good practice to undertake a preliminary evaluation of the array response when the survey is planned. Irregular configurations of even only a few sensors should be preferred, because they allow one to obtain a good compromise between a large aperture, which is necessary for sharp main peaks in the  $EP_b$  and  $EP_m$ , and small inter-sensor distances, which are needed for large aliasing periods (Kind et al., 2005).

Figure 13 shows an example of a suitable 2D array configuration, its respective array response function, and aims by a simple example to clarify a basic aspect related to the array response function role and importance. In fact, Figure (13b) depicts the ideal  $f$ - $k$  plot related to a 5 Hz wave with velocity of 300 m/s, and an optimal distribution of sensors and of seismic sources in far-field (*left panel*), the array response function (*middle panel*), and the convolution of the two (*right panel*). In particular, the latter plot is the  $f$ - $k$  image that can be effectively estimated using a finite number of sensors and the selected geometry in the optimal noise free data-set case. Actually, comparing the ideal (*left panel*) and experimental (*right panel*)  $f$ - $k$  images it is clear that the use of a limited number of sensors introduces blurring effects. As discussed in Picozzi et al. (2010b), the removal by deconvolution of the array response from the  $f$ - $k$  estimates can improve the phase-velocity estimation, reducing the relevant level of uncertainty.

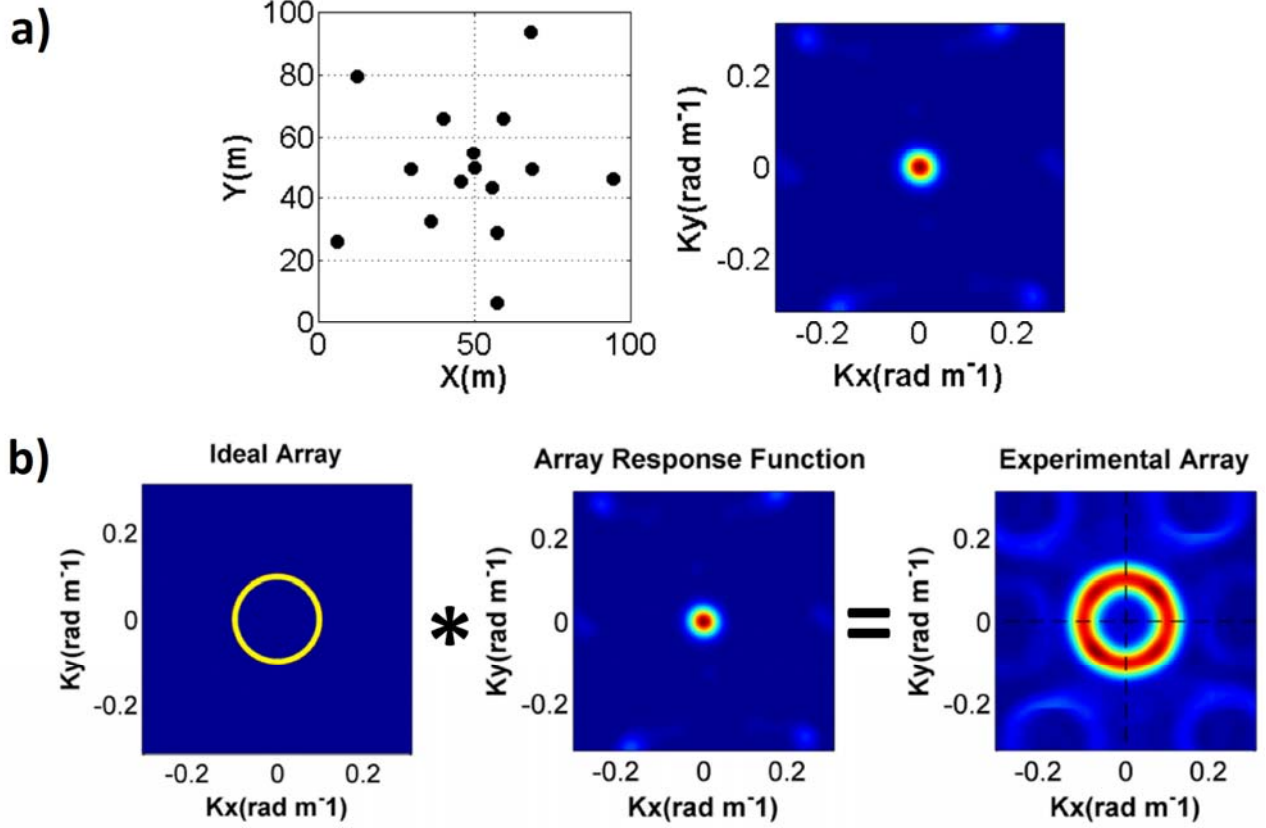


**Figure 13** – a) Array geometry (left panel), and array response function (right panel). b) Ideal array  $f$ - $k$  estimate (left panel), array response function (middle panel), and experimental  $f$ - $k$  estimate (right panel), for a 5 Hz wave.

It is worth noting that the array transfer function is also a powerful tool for the planning of surface wave surveys. Indeed, once the array geometry is designed, it is possible to evaluate *a priori* the array resolution with respect to large wavelengths, and the aliasing related to short wavelengths. Figure 14a shows for the array configuration of Figure 13a an example of poor resolution with respect to a 1 Hz wave with 300 m/s velocity. That is to say, within the experimental  $f$ - $k$  image resulting from the convolution of the ideal  $f$ - $k$  spectra and the array response function (Figure 14a, right panel) it is not possible to identify the ideal circle of wavenumbers related to the wave propagation, but rather a unique wide peak with the maximum in the centre of the  $f$ - $k$  image corresponding to infinite velocity.

On the other hand, Figure 14b depicts for the same array configuration the aliasing effects hampering the  $f$ - $k$  spectra image for a 30 Hz wave and 300 m/s velocity. In fact, for such a short wavelength, the final  $f$ - $k$  image (Figure 14b, right panel) starts to be corrupted by aliasing related artefacts that make it difficult to identify the correct wave velocity.

It is worth noting that given an array configuration, it is straightforward to exploit the array transfer function for identifying those wavelengths (i.e., combinations of phase velocities and frequencies) for which the array resolution is not adequate or those affected by aliasing (Figure 14c). This aspect has to be carefully taken into account for planning the surveys, considering that the size of the array has to be specifically tuned for the frequency range of interest.

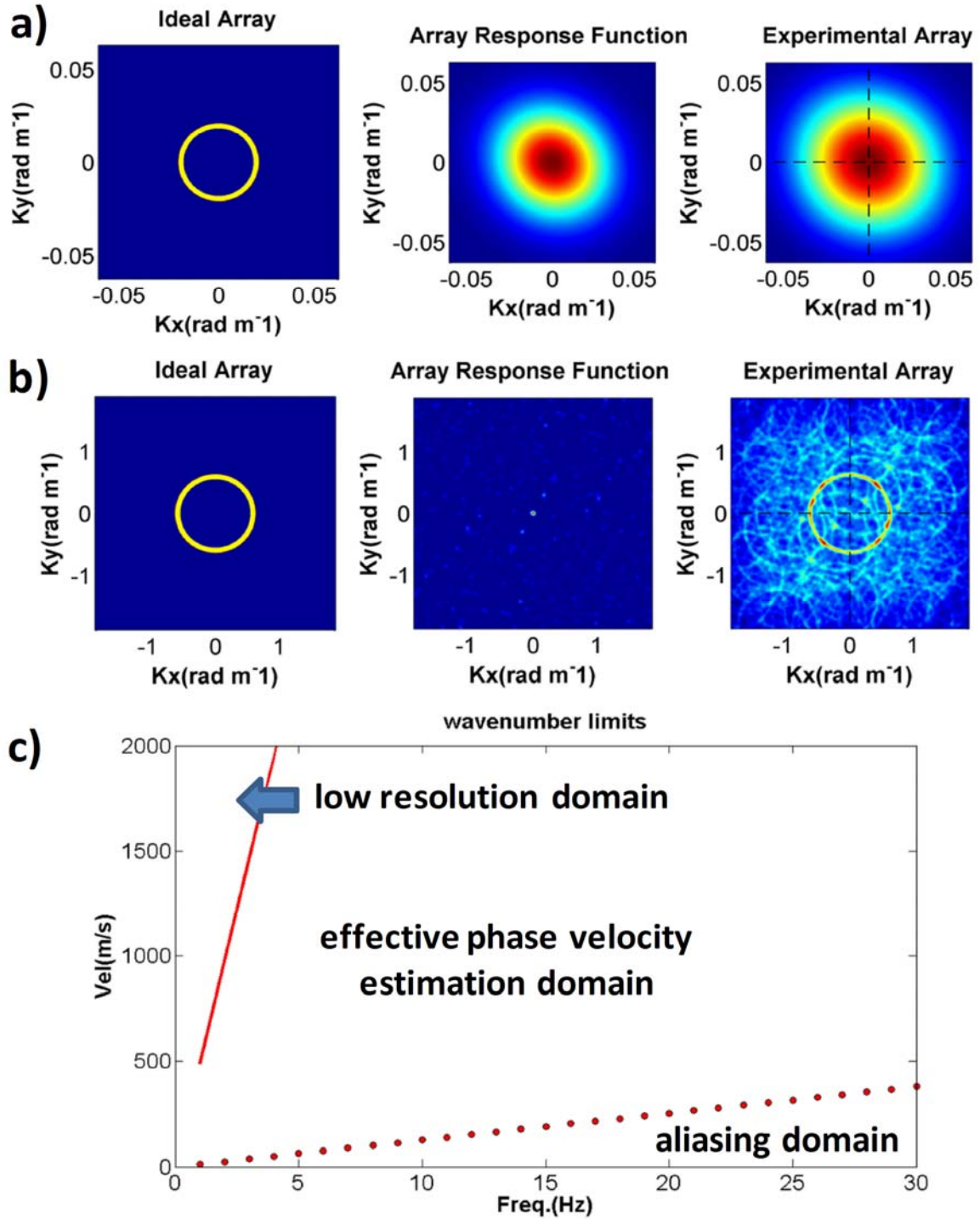


**Figure 14** – a) The same as Figure 13b, but for a 1 Hz wave. b) The same as Figure 13b, but for a 30 Hz wave.

#### 4.2.2. SPatial Auto-Correlation (SPAC) and Extended Spatial Auto-Correlation (ESAC)

Aki (1957,1965) showed that phase velocities in sedimentary layers can be determined using a statistical analysis of ambient noise. He assumed that noise represents the sum of waves propagating without attenuation in a horizontal plane in different directions with different powers, but with the same phase velocity for a given frequency. He also assumed that waves with different propagation directions and different frequencies are statistically independent. A spatial correlation function can therefore be defined as

$$\phi(r, \lambda) = \langle u(x, y, t)(x + r \cos(\lambda), y + r \sin(\lambda), t) \rangle \quad (12)$$

where  $u(x, y, t)$  is the velocity observed at point  $(x, y)$  at time  $t$ ;  $r$  is the inter-station distance;  $\lambda$  is the azimuth and  $\langle \rangle$  denotes the ensemble average. An azimuthal average of this function is given by

$$\phi(r) = \frac{1}{\pi} \int_0^\pi \phi(r, \lambda) d\lambda \quad (13)$$

For the vertical component, the power spectrum  $\phi(\omega)$  can be related to  $\phi(r)$  via the zeroth order Hankel transform

$$\phi(r) = \frac{1}{\pi} \int_0^\infty \phi(\omega) J_0\left(\frac{\omega}{c(\omega)} r\right) d\omega \quad (14)$$

where  $\omega$  is the angular frequency,  $c(\omega)$  is the frequency-dependent phase velocity, and  $J_0$  is the zero order Bessel function. The space-correlation function for one angular frequency  $\omega_0$ , normalized to the power spectrum, will be of the form

$$\phi(r, \omega_0) = J_0\left(\frac{\omega_0}{c(\omega_0)} r\right) \quad (15)$$

By fitting the azimuthally averaged spatial correlation function obtained from measured data to the Bessel function, the phase velocity  $c(\omega_0)$  can be calculated. A fixed value of  $r$  is used in the spatial autocorrelation method (SPAC). However, Okada (2003) and Ohori et al. (2002) showed that, since  $c(\omega)$  is a function of frequency, better results are achieved by fitting the spatial-correlation function at each frequency to a Bessel function, which depends on the inter-station distances (extended spatial autocorrelation, ESAC). For every couple of stations the function  $\phi(\omega)$  can be calculated in the frequency domain by means of (Malagnini et al., 1993; Ohori et al., 2002; Okada, 2003):

$$\phi(\omega) = \frac{\frac{1}{M} \sum_{m=1}^M \text{Re}(S_{jn}(\omega))}{\sqrt{\frac{1}{M} \sum_{m=1}^M S_{jj}(\omega) \sum_{m=1}^M S_{nn}(\omega)}} \quad (16)$$

where  $S_{jn}$  is the cross-spectrum for the  $m$ th segment of data, between the  $j$ th and the  $n$ th station;  $M$  is the total number of used segments. The power spectra of the  $m$ th segments at station  $j$  and station  $n$  are  $S_{jj}$  and  $S_{nn}$ , respectively.

The space-correlation values for every frequency are plotted as a function of distance, and an iterative grid-search procedure can then be performed using equation (20) in order to find the value of  $c(\omega_0)$  that gives the best fit to the data. The tentative phase velocity  $c(\omega_0)$  is generally varied over large intervals (e.g. between 100 and 3000 m/s) in small steps (e.g. 1 m/s). The best fit is achieved by minimizing the root mean square (RMS) of the differences between the values calculated with equation (16) and (15). Data points, which differ by more than two standard deviations from the value obtained with the minimum-misfit velocity, can be removed before the next iteration of the grid-search. Parolai et al., (2006) using this procedure allowed a maximum of three grid-search iterations. An example of the application of this procedure is shown Figure 15.

The ESAC method was adopted to derive the phase velocities for all frequencies composing the Fourier spectrum of the data. Figure 15 (top) shows examples of the space-correlation values computed from the data together with the Bessel function they fit best to. Figure 15 (bottom) shows corresponding RMS errors as a function of the tested phase velocities, exhibiting clear minima. For high frequencies, the absolute minimum sometimes corresponds to the minimum velocity chosen for



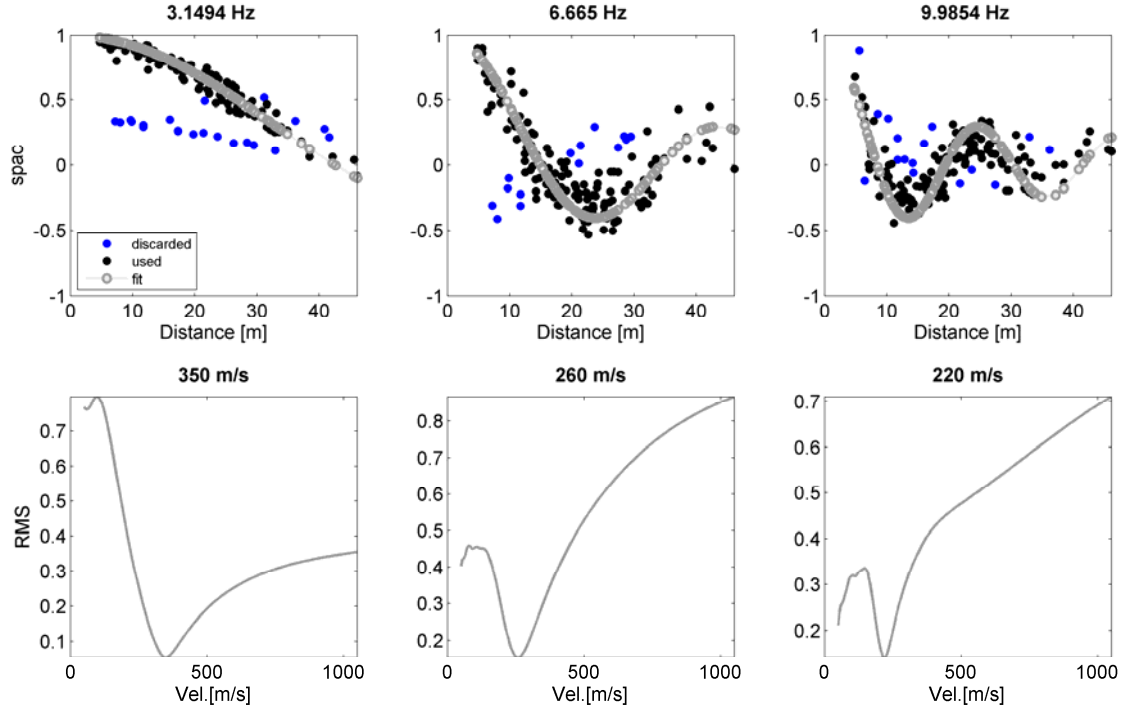


**Figure 15** – Top: Measured space-correlation function values for different frequencies (black and blue circles) and the best-fitting Bessel function (gray circles). Discarded values (blue circles) lie two standard deviations outside the curve. Bottom: The respective RMS error versus phase velocity curves.

the grid search procedure. This solution is then discarded, because a smooth variation of the velocity between close frequencies is required. At frequencies higher than a certain threshold, the phase velocity might increase linearly. This effect is due to spatial aliasing limiting the upper bound of the usable frequency band. It depends on the S-wave velocity structure at the site and the minimum inter-station distance. At low frequencies, the RMS error function clearly indicates the lower boundary for acceptable phase velocities, but might not be able to constrain the higher ones (a plateau can appear in the RMS curves). The frequency, from which phase differences cannot be resolved any more, depends on the maximum inter-station distance and the S-wave velocity structure below the site where a wide range of velocities will then explain the observed small phase differences. Zhang et al. (2004) clearly pointed out this problem in Equation (3a) of their article.

Figure 16 shows examples of the final ESAC dispersion curve compared with those obtained from the  $f$ - $k$  BMF and MLM analyses. Interestingly, all curves in this example look normally dispersive and are in good agreement with each others over a wide range of frequencies. However, at lower frequencies (i.e., below 5 Hz) the  $f$ - $k$  methods provide larger estimates of phase velocity than ESAC. This point was originally discussed by Okada (2003), who defined this ‘ $f$ - $k$  degeneration effect’ and concluded that  $f$ - $k$  methods are able to use wavelengths up two to three times the largest interstation distance, whereas with the ESAC method one may investigate wavelengths up to 10 to 20 times the largest interstation distance, being therefore more reliable in the low-frequency range.

Over the last decade, new developments in SPAC method based on the use of few stations and circular arrays have been proposed with the aim of extracting the Rayleigh and Love wave dispersion velocities (see among the others, Tada et al., 2006; Asten, 2006; García-Jerez et al. 2008).

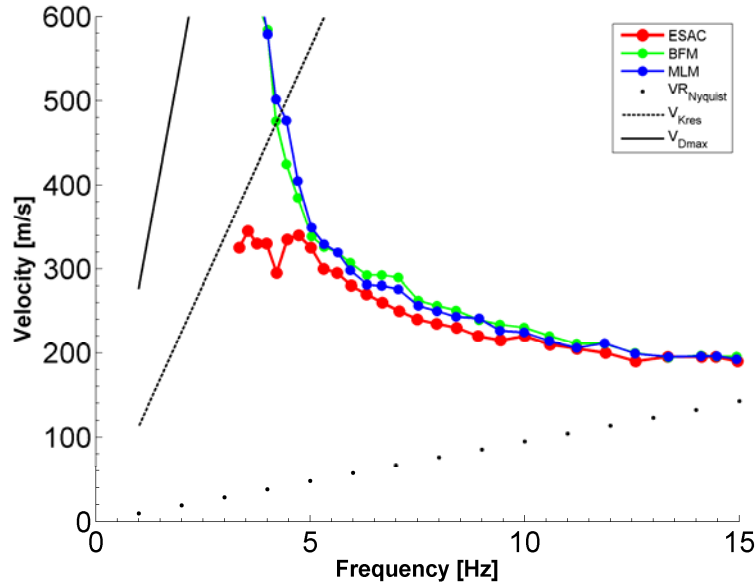


**Figure 16** – Phase velocity dispersion curves obtained by ESAC (reds line), MLM (blue line) and BFM (green line) analysis. The dotted line indicates the theoretical aliasing limit calculated as  $4 \cdot f_{dmin}$ , where  $dmin$  is the minimum interstation distance. The factor 4 is used instead of the generally used factor 2, because the minimum distance in the array is appearing only once. The dashed gray line indicates the lower frequency threshold of the analysis based on  $2 \cdot \pi \cdot f \cdot \Delta k$ , where  $\Delta k$  is calculated as the half-width of the main peak in the array response function. The continuous grey line indicates the lower frequency threshold of the analysis based on the criterion  $f \cdot dmax$ , where  $dmax$  is the maximum interstation distance in the array.

### 4.3. Seismic Noise Horizontal-to-Vertical spectral ratio NHV

In 1989 Nakamura (Nakamura, 1989) revised the Horizontal-to-Vertical (H/V) spectral ratio of seismic noise technique, first proposed by Nogoshi and Igarashi (1970, 1971). The basic principle is that average spectral ratios of ambient vibrations in the horizontal and vertical directions at a single site could supply useful information about the seismic properties of the local subsoil. Since then, in the field of site effect estimation, a large number of studies using this low cost, fast and therefore, attractive, technique have been published (e.g., Field and Jacob, 1993; Lermo and Chavez-Garcia, 1994; Mucciarelli, 1998; Bard, 1998; Parolai et al., 2001). However, attempts to provide standards for the analysis of seismic noise have only recently been carried out (Bard, 1998; SESAME, 2003; Picozzi et al., 2005a). An analogous approach was also proposed by considering earthquake records (Lermo and Chavez-Garcia, 1993), but, being not directly related to surface waves analysis (at least in its original form) it will not be discussed here.

Theoretical considerations (e.g., Tuan et al., 2011) and numerical modelling (e.g., Lunedei and Albarello, 2010) suggest that the pattern of the H/V ratios vs. frequency (NHV curve) presents a complex relationship with subsoil major features. On the other hand, most researchers, on the basis of comparison of noise H/V spectral ratios and earthquake site response, agree that, at least with respect to simple stratigraphic configurations, the maximum of the NHV curve provides a fair estimate of the fundamental resonance frequency of a site. This parameter is directly linked to the thickness of the soft sedimentary cover and this makes NHV curves an effective exploratory tool for seismic microzoning studies and geological surveys.

Recent studies (Yamanaka et al., 1994; Ibs-von Seht and Wohlenberg, 1999; Delgado et al., 2000a, b; Parolai et al., 2001; D'Amico et al., 2008) showed that noise measurements can be used to map the thickness of soft sediments. Quantitative relationships between this thickness and the fundamental resonance frequency of the sedimentary cover, as determined from the peak in the



NHV spectral ratio were calculated for different basins in Europe (e.g., Ibs-von Seht and Wohlenberg, 1999; Delgado et al., 2000 a).

The approach is based on the assumption that in the investigated area, lateral variations of the S-wave velocity are minor and that it mainly increases with depth following a relationship such as

$$v_s(z) = v_{s0}(1 + Z)^x \quad (17)$$

where  $v_{s0}$  is the surface shear wave velocity,  $Z=z/z_0$  (with  $z_0=1$  m) and  $x$  describes the depth dependence of velocity. Taking this into account and considering the well-known relation among  $f_r$  (the resonance frequency), the average S-wave velocity of soft sediments  $\bar{V}_s$ , and its thickness  $h$ ,

$$f_r = \bar{V}_s / 4h \quad (18)$$

the dependency between thickness and  $f_r$  thus becomes

$$h = \left[ v_{s0} \frac{(1-x)}{4f_r} + 1 \right]^{1/(1-x)} \quad (19)$$

where  $f_r$  is to be given in Hz,  $v_{s0}$  in m/sec and  $h$  in m.

Moreover, from (19), an empirical relationships between  $f_r$  and  $h$  is expected in the approximate form

$$h = a f_r^b \quad (20)$$

that can be parameterized from empirical observations, generally applying grid search procedures.

The above approximate interpretation can be easily extended to the case of a two-layer sedimentary cover (D'Amico et al., 2008). Despite the fact that relatively large errors affect the depth estimates provided by this approach (D'Amico et al., 2004), it can be considered as a useful proxy for exploratory purposes.

A possible limitation of this approach is the presence of thick sedimentary covers. In this case, NHV peaks could occur at very low frequency, i.e., below the minimum frequency that can be actually monitored by the available experimental tools. It is worth noting, however, that the generally available seismological/geophysical equipment allows detection of eventual NHV maxima occurring above 0.1-0.5 Hz (see for a detailed discussion about this issue and how to address a priori the choice of the equipment, Strollo et al., 2008). However, considering realistic Vs profiles for soft sedimentary covers, resonance frequencies at or below these frequency values correspond to thicknesses of several hundred meters. In these cases, lithostatic loads provide a strong compaction of sediments, with an expected increase of the relevant rigidity and corresponding Vs value at depth up to values similar to those of the underlying bedrock. This implies that impedance contrasts at the bottom of a thick sedimentary cover tend to become vanishingly small. This implies that such a structural configuration might become of minor interest when looking for amplification effects (but not for variations of ground motion). However, for general microzonation purposes, since the existence of large impedance contrasts at large depths might not be known a priori, and examples of existing large impedance contrast at depth are known in the literature (e.g., Parolai et al., 2001; Parolai et al., 2002), it is advisable that the used equipment are selected considering their technical characteristics that can, a priori, identify frequency bands where only under certain high noise level conditions the fundamental resonance frequency peak can be estimated (Strollo et al., 2008). Furthermore, when geological surveys are of concern, the effect of instrument band width limitations could lead to ambiguous interpretation of a flat NHV curve (outcropping bedrock or very deep sedimentary cover?). Local geological indications in this case could help in identifying the most reliable interpretation.

## 5. Inversion methods

### 5.1. The forward modelling of the Rayleigh wave dispersion curve

The basic element of the inversion procedure is the availability of a fast and reliable tool for solving the forward problem. Theoretical modelling suggests that the dispersion curves of the fundamental and higher mode Rayleigh waves and the NHV spectral ratio, while mainly depending on the S-wave velocity structure, are dependent on also the density and P-wave velocity structure. Concerning the damping profile, numerical experiments indicate that the sensitivity of the Rayleigh and Love waves dispersion curve results are relatively weak, while the NHV curve is much more sensitive to this parameter (Lunedei and Albarello, 2009).

Several procedures exist to compute expected surface waves amplitudes and propagation velocities (both for the fundamental and higher modes) in the case of a flat weakly or strongly dissipative layered Earth (e.g., Buchen & Ben-Hador 1996; Lai and Rix, 2002). In general, modal characteristics of surface waves are provided in implicit form (zeroes of the normal equation) and this implies that numerical aspects play a major role (e.g., Lai and Wilmanski, 2005). Thus, the effectiveness of available numerical protocols (e.g., Herrmann, 1987) mainly relies on their capability in reducing numerical instabilities (mode jumping, etc.).

In order to simplify the problem, the dominance of a fundamental propagation mode is commonly assumed. However, several studies (e.g., Tokimatsu et al., 1992; Foti, 2000; Zhang and Chan, 2003; Parolai et al., 2006) showed that for sites with S-wave velocities varying irregularly with depth (low velocity layers embedded between high velocity ones) a higher mode or even multiple modes dominate certain frequency ranges. This results in an inversely dispersive trend in these frequency ranges. Therefore, due to the contribution of higher modes of Rayleigh waves, the obtained phase velocity has to be considered an apparent one. Moreover, other studies (Karray and Lefebvre, 2000) showed that even at sites with S-wave velocity increasing with depth, the fundamental mode does not always dominate (see also section 2.2). Tokimatsu et al. (1992) formulated the apparent phase velocity derived from noise-array data as the superposition of multiple-mode Rayleigh waves. Ohori et al. (2002) adopted this formulation making use of the method of Hisada (1994) for calculating the dispersion curves. Assuming that source and receivers are located only at the surface, Tokimatsu et al. (1992) proposed that the apparent phase velocity is related to the multiple-mode Rayleigh waves through:

$$c_{si}(f) = 2\pi fr \left\{ \cos^{-1} \left[ \frac{\sum_{m=0}^M A_m^2(f) c_m(f) \cos\left(\frac{2\pi fr}{c_m(f)}\right)}{\sum_{m=0}^M A_m^2(f) c_m(f)} \right] \right\}^{-1}, \quad (21)$$

where  $c_{si}(f)$  is the apparent phase velocity,  $c_m(f)$  and  $A_m(f)$  are the phase velocities of the  $m$ th Rayleigh wave mode and the corresponding medium response (Harkrider, 1964).  $A_m(f)$  is related to the power spectrum density function of the  $m$ th mode,  $M$  is the maximum order of mode for each frequency, and  $r$  is the shortest distance between sensors. Parolai et al. (2006) confirmed that in the case of subsoil profiles with low velocity layers leading to apparent dispersion curves, the inversion carried out by only considering fundamental modes yielded artifacts in the derived S-wave velocity profiles.

The presence of higher modes is also responsible for another problem. The number of existing modes depends on the frequency (Aki and Richards, 1980): this implies that, depending on the subsoil structure, abrupt changes exist in this number as a function of frequency (modal truncation). In particular, when higher modes play a significant role, their sudden disappearance results in

unrealistic jumps in the computed dispersion and NHV curves. To reduce this problem, as suggested by Picozzi and Albarello (2007), a number of fictitious very thick layers (of the order of km) have to be added below the model to prevent artefacts. Of course, the parameters of these layers cannot be resolved by the experimental curves and simply have the role of preventing modal truncation effects.

Beyond these problems, one should be aware that surface waves only represent a part of the existing wave field. Other seismic phases (near field, body waves) also exist and could play a major role. During active surveys, this problem could be resolved by selecting suitable source-receiver distances. However, when passive procedures are of concern, it is not possible to select suitable sources and some problems could arise. In general, seismic array procedures (*f**k*, ESAC, SPAC) allow to individuate and to remove the effect of such waves. However, this cannot be done in a single station setting (NHV). These effects have been explored theoretically (Albarello and Lunedei, 2010; Lunedei and Albarello, 2010) by modelling the average complete noise wave field generated by surface point sources. This study revealed that the surface waves solution only holds (above the fundamental resonance frequency of a site) in the case where a source free area of the order of several tens to hundreds meters (depending on the subsoil configuration) exists around the receiver.

As discussed from section 1, surface wave dispersion analyses rely on the basic assumption that the medium can be approximated by 1D geometry; that is to say, isotropic and laterally homogeneous layers. Of course, any violation from this assumption, such as the presence of lateral heterogeneities in the subsoil structure, makes the forward modelling discussed inadequate. In general, lateral velocity variations dramatically affect both amplitudes and propagation velocities. However, it can be shown (e.g., Snieder, 2002) that when the wavelength of concern is much larger than the horizontal scale length of the structural variation, *local modes* can be considered. These are defined at each horizontal location (*x*, *y*) as the modes that the system would have if the medium would be laterally homogeneous. That is, the properties of the medium at that particular location (*x*, *y*) can be considered to be extended laterally infinitely. In this approximation, 1D models can be applied, making it possible to develop approximate surface waves tomographic approaches (Picozzi et al., 2008).

## 5.2. The forward modelling of Horizontal-to-Vertical Spectral Ratio curve

Arai and Tokimatsu (2000, 2004) proposed an improved forward modelling scheme for the calculation of NHV spectral ratios. Moreover, this scheme has been successfully applied in a joint inversion scheme of NHV and dispersion curves by Parolai et al. (2005), Arai and Tokimatsu (2005), Picozzi and Albarello (2007), and D'Amico et al. (2008).

Arai and Tokimatsu (2000) showed that NHV spectral ratios can be better reproduced if the contribution of higher modes of Rayleigh waves and Love waves is also taken into account. They suggest to calculate the NHV spectral ratio as:

$$(\text{NHV})_s = (P_{\text{HS}}/P_{\text{VS}})^{1/2} \quad (22)$$

where the subindex *s* stands for surface waves, and  $P_{\text{VS}}$  and  $P_{\text{HS}}$  are the vertical and horizontal powers of surface waves (Rayleigh and Love), respectively.

The vertical power of the surface waves is only determined by the vertical power of the Rayleigh waves ( $P_{\text{VR}}$ ), while the horizontal power must consider the contribution of both Rayleigh ( $P_{\text{HR}}$ ) and Love waves ( $P_{\text{HL}}$ ). The following equations can therefore be used:

$$P_{\text{VS}} = P_{\text{VR}} = \sum_j (A_{Rj}/k_{Rj})^2 \left\{ 1 + (\alpha^2/2)(u/w)_j^2 \right\} \quad (23)$$

$$P_{HS} = P_{HR} + P_{HL} \quad (24)$$

$$P_{HR} = \sum_j \left( A_{Rj} / k_{Rj} \right)^2 (u/w)_j^2 \left\{ 1 + (\alpha^2/2) (u/w)_j^2 \right\} \quad (25)$$

$$P_{HL} = \sum_j \left( A_{Lj} / k_{Lj} \right)^2 (\alpha^2/2) \quad (26)$$

where  $A$  is the medium response,  $k$  is the wavenumber,  $u/w$  is the H/V ratio of the Rayleigh mode at the free surface,  $j$  is the mode index, and  $\alpha$  is the H/V ratio of the loading horizontal and vertical forces  $L_H/L_V$ . Parolai et al. (2005) and Picozzi et al. (2005b) showed that varying  $\alpha$  over a large range did not significantly change the NHV shape. Therefore, they used  $\alpha=1$ .

A basic problem of these inversion procedures is the choice of frequency band to be considered for the inversion of the NHV curve. As an example, the NHV values around the maximum have been discarded by Parolai et al. (2006) and instead taken into account by Picozzi and Albarello (2007) and D'Amico et al. (2008). Recent theoretical studies (Lunedei and Albarello, 2010; Albarello and Lunedei, 2010; Tuan et al., 2011) indicated that the NHV curve around the fundamental resonance frequency  $f_0$  (i.e., around the NHV maximum) can be significantly affected by the damping profile in the subsoil and by the distribution of sources around the receiver. In particular, they showed that sources located within a few hundred meters of the receiver can generate seismic phases that strongly affect the shape of the NHV curve around and below  $f_0$ . This implies that, unless a large source-free area exists around the receiver, the inversion of the NHV shape (around and below  $f_0$ ) carried out using forward models based on surface waves only, might provide biased results.

### 5.3. Inversion procedures

The inversion task can be accomplished with a number of strategies. A first order strategy classification of inversion procedures is between Local Search Methods (LSM) and Global Search Methods (GSM). A wide variety of local and global search techniques have been proposed to solve the non-linear inverse problem. In this work we will briefly outline the following: the Linearized Inversion, the Simplex Downhill Method (Nelder and Mead, 1965), the Monte Carlo approach and the Genetic Algorithm (e.g. Goldberg, 1989). Other global search methods proposed for surface wave dispersion inversion are: the Simulated Annealing (Beatty et al., 2002), the Neighbourhood Algorithm (Sambridge, 1999a, b; Wathelet et al., 2004), and the Coupled Local Minimizers (Degrande et al., 2008).

#### 5.3.1. Linearized Inversion (LIN)

As previously discussed, when linearized inversion methods are used, the final model inherently depends on an assumed initial model because of the existence of local optimal solutions. When an appropriate initial model is generated using a-priori information about the subsurface structure, linearized inversions can find an optimal solution that is the global minimum of a misfit function.

The inverse problem is generally solved using Singular Value Decomposition (SDV, Press et al., 1986) and the Root Mean Square (RMS) of differences between observed and theoretical phase velocities (or in case of single station measurements, between observed and theoretical NHV) are minimized. Because of the non-linearity of the problem, the inversion is repeated until the RMS ceases to change significantly. Also, iterative inversion techniques like the simultaneous iterative reconstruction technique (Van der Sluis and Van der Vorst, 1987) are used, but they do not provide any advantage with respect to using SVD.

### 5.3.2. Simplex Downhill Method (SDM)

Ohori et al. (2002) proposed using the SDM method originally outlined by Nelder and Mead (1965) to minimize the discrepancy between the squared differences of observed and theoretical phase velocities, normalized to the squared value of the observed velocities. For multi-dimensional minimizations, the algorithm requires an initial estimate. Generally, two chosen starting points are provided. The solution with the minimum misfit is adopted and the inversion then repeated, restarting from this solution. The SDM quickly and easily locates a minimum, even if, however, it might miss the global one.

### 5.3.3. MonteCarlo Method (MC)

In Monte Carlo (MC) procedures (Press, 1968; Tarantola, 2005) the space of model parameters is randomly explored and the numerical dispersion curves associated with each of several possible shear wave velocity profiles compared to the experimental dispersion curve. In contrast to linearized inversions schemes, *MC* inversion schemes require only an evaluation of the functions, not their derivatives. One of the main problems is the need to explore a sufficient number of profiles in order to obtain an adequate sampling of the model parameters space. An efficient inversion algorithm for the inversion of surface wave data makes use of the scale properties of the dispersion curves (Socco and Boiero, 2008). These properties are linked to the scaling of the modal solution with the wavelength. If model parameters are scaled, the corresponding modal dispersion curve scales accordingly. In particular, both the phase velocities and frequencies scale if all the layer velocities are scaled, while only the frequencies scale if all the layer thicknesses are scaled (Socco and Strobbia, 2004). A multimodal Monte Carlo inversion based on a modified misfit function (Maraschini et al., 2010) has been recently proposed by Maraschini and Foti (2010).

### 5.3.4. Modified Genetic Algorithm (GA)

With this algorithm, a search area is defined for both the S-wave velocity and thickness of the layers. An initial population of a limited number of individuals (e.g., 30) is generated and genetic operations are applied in order to generate a new population of the same size. This new population is reproduced based on a fitness function for each individual (Yamanaka and Ishida, 1996). For surface wave inversion, the fitness function can be defined considering the average of the differences between the observed and the theoretical phase velocities. In addition to the crossover and mutation operation, two more genetic operations can be used to increase convergence, namely elite selection and dynamic mutation. Elite selection assures that the best model appears in the next generation, replacing the worst model in the current one. To avoid a premature convergence of the solution into a local minimum, the dynamic mutation operation was used to increase the variety in the population. Therefore, GA is a non-linear optimization method that simultaneously searches locally and globally for optimal solutions by using several models (Parolai et al., 2005).

Since this inversion applies a probabilistic approach using random numbers and finds models near to the global optimal solution, it is repeated several times by varying the initial random number. The optimal model is selected considering the minimum of the chosen fitness function. Recently, Picozzi and Albarello (2007) suggested to combine the GA inversion with a linearised one. In practice, the linearized inversion is started by using as the input model the best model of the GA inversion that it is supposed to be located close to the global minimum solution.

### 5.3.5. Rayleigh wave dispersion curve inversion

Parolai et al. (2006) compared different algorithms for the inversion of Rayleigh wave dispersion curves using a data-set of seismic noise recordings from different sites in the Cologne area. In particular, these authors considered the linearized inversion (e.g., Tokimatsu *et al.*, 1991), the simplex downhill method (Nelder and Mead, 1965), and the non-linear optimization method that uses a genetic algorithm (e.g., Goldberg, 1989).

Figure 17 shows the inversion results for the different methods. Parolai et al. (2006) showed that when constraining the total thickness of the sedimentary cover from geological and geotechnical information, linearized local search inversions can provide very similar results to those from global search methods. However, in an area with a completely unknown structure, the genetic algorithm inversion is the preferred method. In fact, although the computations are more time-consuming, this method is less dependent upon a priori information, hence making this inversion scheme the most appealing method for deriving reliable S-wave velocity profiles.

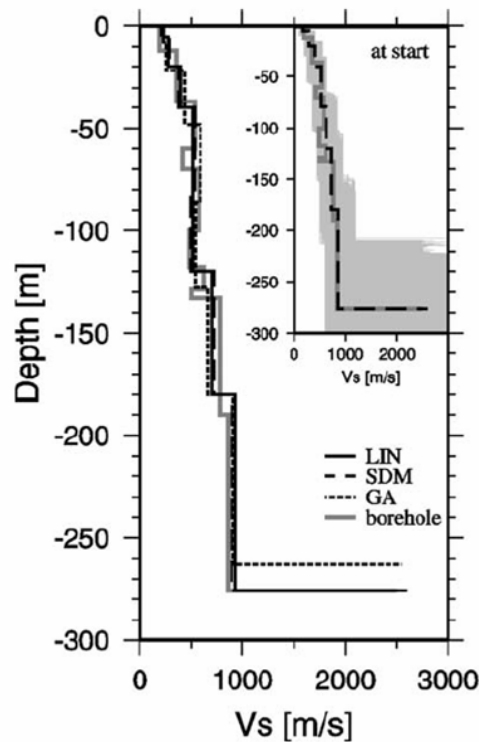


**Figure 17** – Results from inverting the apparent Pulheim dispersion curve. The insets show the starting model for LIN and SDM (dashed), together with the borehole model. Light gray indicates the models tested in the GA inversion. Note that the S-wave velocity in the bedrock of the tested models varied by up to 3300 m/s (data from Parolai et al., 2006).

### 5.3.6. NHV inversion

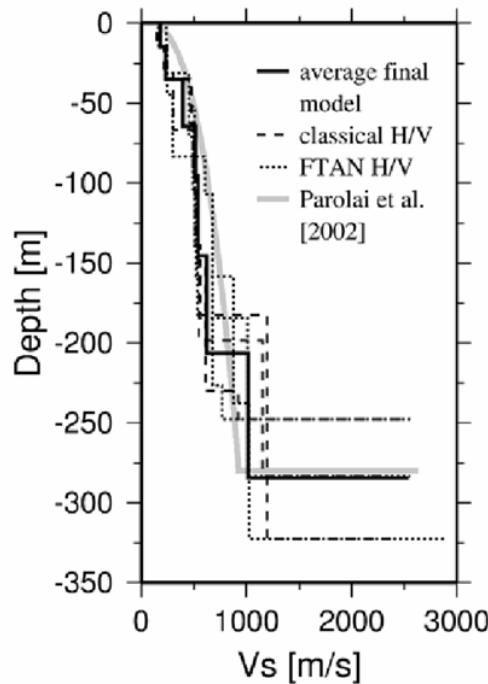
The possibility of retrieving the S-wave velocity structure below a site from single station measurements based on NHV ratio computation was tested by Fäh et al. (2001). They suggested a new method for calculating NHV ratios employing a time-frequency analysis (FTAN). Moreover, after having shown that there is a good agreement between the NHV ratio and the theoretical ellipticity curves of the fundamental mode Rayleigh wave, they proposed to invert the NHV curve to derive directly the S-wave subsoil structure. The NHV was corrected for the contamination by SH and Love waves by simply reducing it by a factor  $\sqrt{2}$ , independent of frequency. The inversion, due to the non-linear nature of the problem, was based on a genetic algorithm (GA) (Fäh et al., 2001,

2003). The inversion was carried out for a fixed number of layers and a-priori defined ranges of the geophysical properties (S-wave, P-wave, density and thickness) of the layers. An initial starting population of individuals was generated through a uniform distribution in the parameter space. The model that, amongst all those generated, allows the best reproduction of the observed NHV, was chosen as the best model.

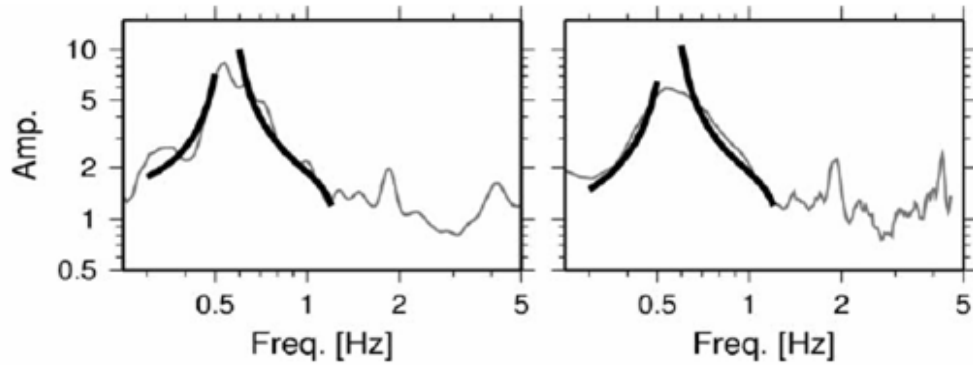
Recently, Tanimoto T. and Alvizuri (2006) and Hobiger et al. (2009) proposed to extract the ellipticity of Rayleigh waves from NHV curves by a random decrement technique. This might in turn be used as input for the inversion analyses to estimate the S-wave velocity profiles.

Figure 18 shows the S-wave velocity profiles obtained by inverting NHV curves (calculated in a standard way and by FTAN) for a site in the Cologne area (Parolai et al., 2006).

The inversion was carried out by fixing the total thickness of the sedimentary cover in order to avoid problems of trade-off between the total thickness and the S-wave velocity (Scherbaum et al., 2003; Arai and Tokimatsu, 2004). Three different values for the total thickness of the sediments were considered: the average value from an empirical relation between velocity versus depth calculated for the investigated area, and the maximum and minimum values considering the standard errors in that relationship. Figure 19 shows the fit to the average NHV ratios. Finally, the derived S-wave velocity profiles have been compared with those obtained by array techniques (Parolai et al., 2006) and an excellent agreement was found.



**Figure 18** – NHV ratio inversion results for the Pulheim site (Cologne). For both the classical and the FTAN methods, results from fixing different sedimentary cover thicknesses (thin/thick sediments) are shown (data from Parolai et al., 2006).



**Figure 19** – Example of average NHV ratios inverted for sites in Cologne: Classical analysis (left) and FTAN method (right). The fundamental mode Rayleigh wave ellipticity calculated for one of the final GA models is indicated in black. (data from Parolai et al., 2006).

In Parolai et al., (2006) the inversion of NHV curves was extended to 20 of the sites measured by Parolai et al. (2001) and a 2D S-wave velocity model was derived by means of interpolating between the derived 20 profiles. Figure 20 shows the resulting 2D S-wave velocity model (bottom) together with a geological cross-section. The agreement between the geological structure and the S-wave velocity model is obviously very good. Compared to the average velocity relationship previously derived for the whole area, lateral variations in the velocity structure are clearly visible.

Therefore, it was shown that given that the bedrock depth can be constrained and the sedimentary cover is fairly regularly layered, the NHV inversion is a suitable method for quickly mapping 3D S-wave velocity structures. The vertical resolution of the profiles was also found to be sufficient to provide site responses (Parolai et al., 2006; 2007) by means of numerical simulations, in agreement with the empirical ones.

### 5.3.7. Joint inversion of Rayleigh wave dispersion and NHV curve

While both dispersion and NHV ratio curves can be singularly inverted to retrieve the local S-wave profile, it has been shown from Scherbaum et al. (2003) that these inversions are hampered by the non-linearity of the data-model parameters relationship. In fact, these authors showed that the NHV ratio and the dispersion curves display different sensitivity to the S-wave velocity and thickness of the sedimentary layers. In particular, the dispersion curve represents the main constraint in the definition of the S-wave velocity of the soft sediments, while the fundamental frequency estimated from the NHV or Rayleigh wave ellipticity peak constrains mainly the total thickness of the sediment cover. Hence, when the inversion is applied to these curves separately, there is an unresolvable trade-off between the model parameters, which hampers the analysis results. To overcome this problem, Parolai et al. (2005) and Arai and Tokimatsu (2005) proposed a joint inversion of phase velocity and NHV ratio curves. They showed that with this approach, the trade-off between the model parameters can be reduced and a reliable evaluation of the local S-wave velocity structure can be obtained.

Figure 21 shows the results obtained by inverting the Cologne data set of dispersion and NHV using the GA scheme (Parolai et al., 2005). The fit of the calculated to the observed data is remarkable for the minimum cost model. For comparison, the fundamental mode Rayleigh wave dispersion curve is also plotted in the top inset of Figure 19. The final model differs from the one calculated by Parolai et al. (2006) using only phase velocities mainly in the total thickness of the sedimentary cover. The authors compared the fit of these two final models to the observed dispersion as well as the H/V ratio curves. The analysis confirmed that with the joint inversion, the dispersion curves are equally well fitted, but the cost function for the H/V ratio curve fit was reduced by more than 50%.



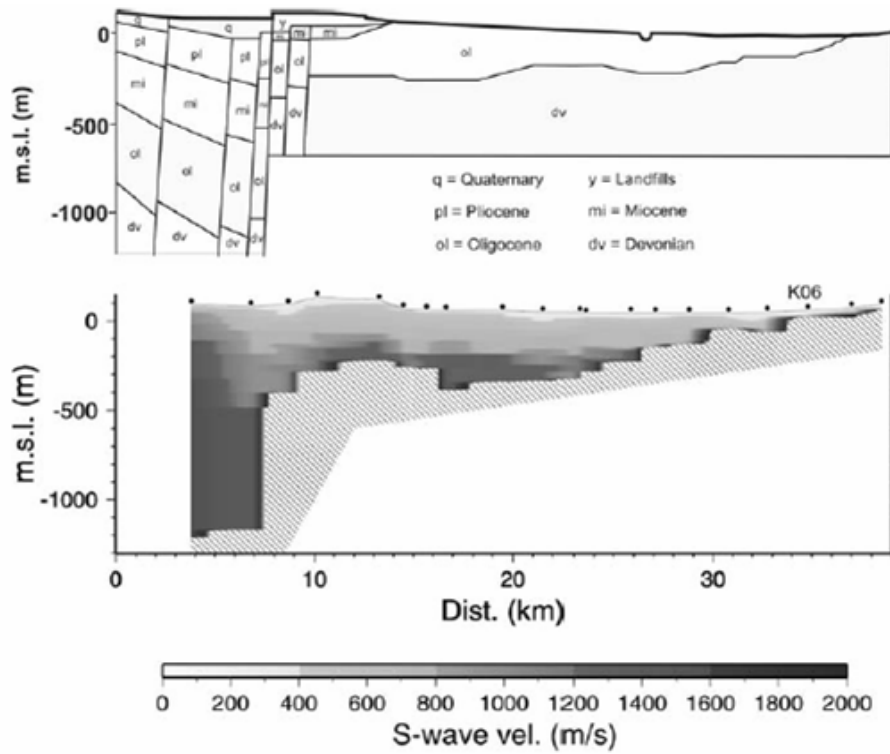


**Figure 20** – Top: Geological cross section of the sedimentary cover in Cologne. Bottom: 2D S-wave velocity model interpolated from 1D S-wave velocity profiles calculated for the 20 selected sites (Parolai et al., 2006). The striped pattern indicates the Devonian bedrock (data from Parolai et al., 2006).

Therefore, the joint inversion allowed the retrieving of a more reliable model of the local velocity structure than by using only dispersion curves.

#### 5.3.8. Two-step Joint inversion of Rayleigh wave dispersion and NHV curves

Despite the fact that both GA and LIN inversion approaches can be effective, in many cases they lead towards non-optimal parametrization. Indeed, in highly ill-posed inversion problems, GA could be stalled by a complicated fitness landscape and be unable to exactly single out the global optimum solution (Mosegaard & Sambridge 2002). On the other hand, when LIN methods are used, poor starting models are likely to result in low-quality or undesired parameter estimation (Menke, 1989).

In order to overcome these difficulties, a possible strategy consists in combining both kinds of inversion methods to benefit from the advantages of each. Hence, Picozzi and Albarello (2007), introduced the idea to perform a two-step inversion scheme of surface wave curves by combining GA and LIN techniques. In particular, in the first step of the analysis, the use of GA allows a non-linear inversion analysis to be performed that does not depend upon an explicit starting model. This is the most straightforward property of GA, considering that site-effect investigations are often required in regions where there is little or no knowledge about the subsurface available. The best-fitting model of GA is then used as the starting model for the LIN inversion that has been able to drive the inversion to the global optimal minimum of the cost function. This results in a model that satisfactorily reproduces, within relevant errors, all the experimental data.

Figure 22 shows the results of this two-step inversion approach when applied to the joint inversion of NHV ratios and Rayleigh wave dispersion curves deduced from environmental noise measurements carried out at a well-known test site located near the Casaglia Village in Northern Italy.

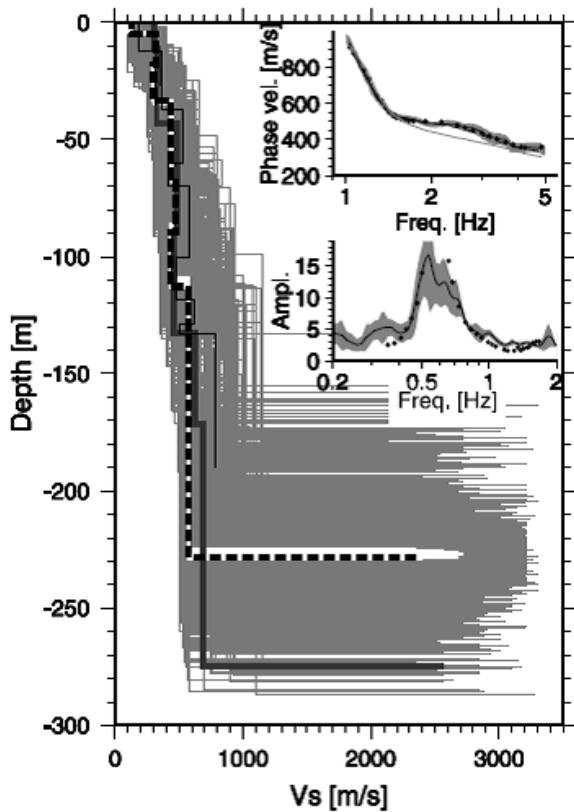


**Figure 21** – Results of the dispersion and NHV joint inversion. Tested models (gray lines), the minimum cost model (dashed line), and models lying inside the minimum cost +10% range (white lines). Top inset: observed phase velocities (black line) and the phase velocities for the minimum cost model (dots). The intervals (gray shading) around the observed phase velocities are obtained by calculating the square root of the covariance of the error function. Bottom inset: average observed H/V ratio (black line)  $\pm 1$  std. dev. (gray shaded area) and the H/V ratio for the minimum cost model (dots). The thick gray line indicates the model obtained by Parolai et al. (2006) inverting only the phase velocity data, while the thin black line shows the measured S-wave velocity in a borehole close to the location. The fundamental mode Rayleigh wave dispersion curve of the minimum cost model is shown (top inset: gray line). Data from Parolai et al., (2005).

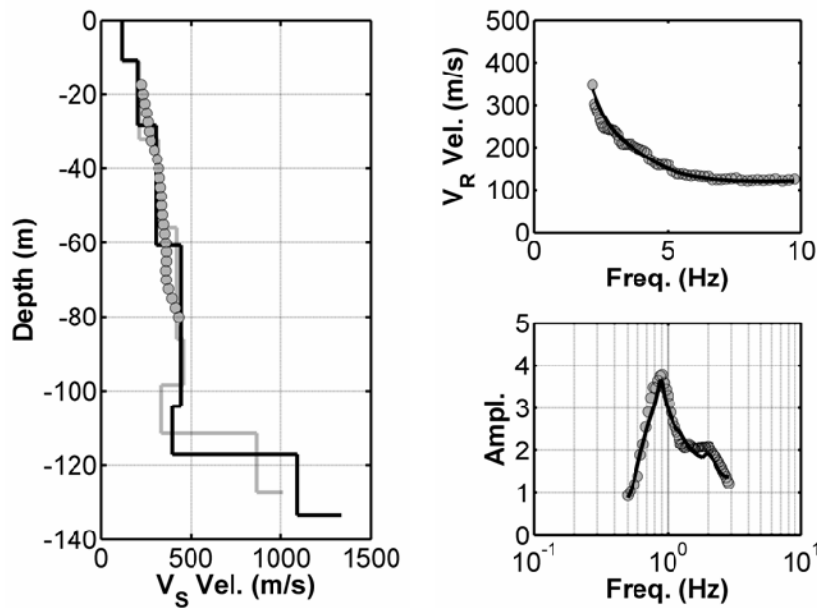


**Figure 22** – Results of the two-step joint inversion carried out with GA and LIN algorithms. (a) S-wave velocity profile from GA inversion (light gray), LIN inversion (black), and CH measurements (gray dots, from Malagnini et al. 1997). (b) Top inset: Experimental (gray dots) and theoretical (black) from LIN inversion Rayleigh wave dispersion curves. Bottom inset: Same as Top inset, but for H/V curves. (modified from Picozzi and Albarello, 2007).

## 6. Recommendations

The choice of specific approaches for acquisition, processing and inversion within each testing technique is strongly linked to available instruments and the specific experience of the operator. Although in principle all methods, if carefully applied, should yield sufficiently reliable results, the following general suggestions can be made:

- ⇒ When active tests are concerned, the 2-station method is not preferable because its interpretation in noisy environment and for complex sites can be very different. In particular, the process of phase unwrapping can lead to substantial errors and requires an experienced operator. Moreover, it has to be considered that the phase difference measurement can be affected by instrumental error and the standard testing procedure (common receiver midpoint) is quite time consuming on site;
- ⇒ As passive tests are concerned, the use of linear arrays and the ReMi method should be avoided because these rely on the strong assumption of the homogeneous distribution of sources and the picking of intermediate points in the f-p (or f-k) spectrum is operator dependent. If ReMi methods are used anyway, it is suggested to combine data acquisition with active MASW data, since the testing setup is the same and only some shots with an active source (for shallow depth of investigation, a sledge hammer will suffice) are required;
- ⇒ For the inversion of surface wave data, the influence of higher modes in the propagation has to be carefully taken into account and the use of global search methods is suggested, especially for sites with more complex geology. If not, there is a higher probability of the experimental dispersion curve being trapped in local minima;

Some specific recommendations concern the application of surface waves prospecting techniques for the characterization of sites on outcropping rock

The seismic characterization of stiff-soil and rock-mass sites (behaving as seismic bedrock) represents a critical aspect for effective and proper location of seismic and accelerometric stations, and for the analysis of seismic response when following the reference station approach. In general, it is assumed that flat rock and stiff soil sites represent an ideal location where possible near surface amplification effects can be excluded. However, this assumption is not consistent with widespread evidence of rock and soil alteration phenomena induced by faulting, jointing and weathering. These phenomena could be responsible for significant modifications of the dynamic properties of the subsoil, both in the vertical direction and laterally. In particular, they can alter the seismic response at the site due to the presence of Vs velocity contrasts.

In general, the presence of vertical variations can be easily revealed by point-wise NHV measurements and the relevant Vs profile can be constrained by jointly inverting NHV and surface wave dispersion curves obtained by array measurements nearby the station. However, as it concerns the latter, some critical aspects should be accounted for. In the presence of relatively high phase velocities (such as the ones expected at stiff and rock-mass sites), large wavelengths with respect to the overall dimensions of the array are expected in the frequency range commonly considered for this kind of analysis (5-20 Hz to say). Thus, relatively small phase differences are expected at most of the array receivers and this adversely affects the resolving power in the velocity domain. Phase velocity measurements, in fact, ultimately depend on the estimate of the phase differences  $\delta\phi$ . By definition, one has

$$\delta\phi = 2\pi\nu\delta t = 2\pi f \frac{x}{V_\nu} \quad (27)$$

where  $V_v$  is the phase velocity at the frequency  $f$  and  $\delta t$  is the time delay between phase arrivals at two sensors located at a distance  $x$  from each other. By this equation, one can relate resolution  $\Delta(\delta\phi)$  in the phase difference domain to the ones in the phase velocity  $\Delta V_v$  and time  $\Delta(\delta t)$  domains, i.e.,

$$\Delta(\delta\phi) \approx 2\pi f \Delta(\delta t) \approx 2\pi r \frac{f}{V_v^2} \Delta V_v \quad (28)$$

Rearranging eq. 28, one obtains

$$\Delta V \approx \frac{V_v^2}{r} \Delta(\delta t) \quad (29)$$

The resolution in the time domain is related to the sampling frequency  $\tau$  and thus,

$$\Delta V \approx \frac{1}{\tau} \frac{V_v^2}{r} \quad (30)$$

This last relationship shows that, keeping fixed the inter-geophonic distance and the sampling rate, the accuracy of the velocity estimates dramatically decreases with increasing phase velocities (Zhang et al., 2004). Furthermore, the smallest inter-geophone distance  $\Delta x_{\min}$  able to provide a velocity value at the sampling frequency  $\tau$  is  $V_v/\tau$ . This implies that aliasing occurs for wavelengths smaller than  $2r_{\min} = 2 V_v/\tau$ : in the case where most of the inter-geophone distances of the array are less than  $2r_{\min}$ , all wavelengths below this value are undersampled from a statistical point of view. The longest resolvable wavelength is of the order of the overall dimension  $D$  of the array and this last dimension also limits the resolving power of the array in the wavenumber domain: this last limitation is more significant as larger are the involved wavelengths and phase velocities. As an effect of these limitations (especially the finiteness of the sampling rate), the dispersion curve deduced from array measurements can assume a characteristic saw-tooth shape that masks the underlying smooth pattern and makes it difficult to make a physically plausible interpretation.

Thus, in order to provide good velocity measurements, one has to increase both the sampling rates and the inter-geophone distances. In general, fewer problems exist in increasing sampling rates, but does raise the concern of the availability of sufficient memory storage when passive measurements are of concern and long measurement sessions are necessary. Much more complex is the problem of providing relatively large arrays to maximize  $r$ . In fact, being more resistant to erosion, the stiff soil sites are characterized in many cases by rough topography that limits the availability of extended flat areas to locate an array. Thus, in general, one should expect that phase velocity estimates deduced for stiff soil/ rock sites are less accurate than those obtained from surveys carried out on soft soil sites. This implies that “robust” techniques should be preferred. As an example, due to the relatively low accuracy of phase velocity determination, the possibility to actually resolve higher modes could be scarce and in some case results in misleading interpretations. Thus, the use of effective phase velocity curves instead of modal curves results more cautionary and can provide more reliable inversions.

Another important problem affecting rock sites is the presence of brittle deformation (faulting) that could be responsible for significant lateral variations in the mechanical properties of the subsoil. These can be detected by exploratory NHV measurements driven by geological features that allow a preliminary mapping of the possibly different dynamical behaviour of geological features around the station. Interferometric interpretation of array measurements could also help in the identification and characterization of existing lateral heterogeneities.

Finally, as a test case example of 2D array measurements carried out on a site with outcropping bedrock, the results obtained by Picozzi et al. (2009) in Istanbul are shown in Figure 23. In

agreement with what has been discussed in this section, due to the high S-wave bedrock velocity and the resultant large wavelengths, the estimation of the Rayleigh wave dispersion curve was possible for a limited range of frequencies only. Despite this limitation, it is worth noting that, when compared with logging surveys, the seismic noise measurements allowed the retrieval of the S-wave velocity structure for some hundreds of meters at the price of a very little investment.

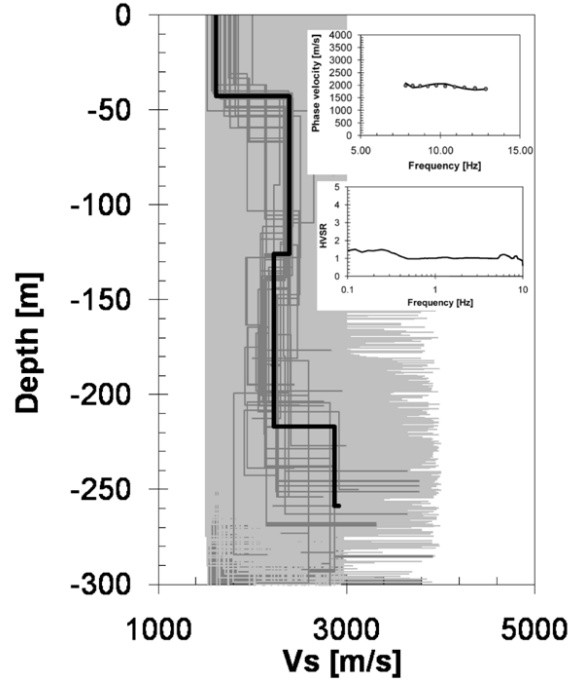


**Figure 23** – Example of inversion results for 2D array measurements carried out on a site with outcropping bedrock in Istanbul. a) Tested models (thin grey lines), the minimum cost model (black line), and models lying inside the minimum cost +10% range (white lines). b) Top inset: Observed phase velocities (grey dots) and the phase velocities for the minimum cost model (black line). Bottom inset: Average observed  $H/V$  ratio (black line), (modified from Picozzi et al, 2009).

## 7. New perspectives: Interferometry and tomography for surveys in 2D/3D sites

Current trends in surface wave methods include attempts to evaluate lateral variations. Often this is pursued with a collection of adjacent surface wave surveys (Tian et al., 2003; Bohlen et al., 2004; Neduczka, 2007). Reinterpretation of seismic reflection/refraction datasets provides a cost effective approach in this respect (Grandjean and Bitri, 2006; Socco et al., 2009). A consistent pseudo-2D shear wave velocity model can be obtained by a single laterally constrained inversion (Auken and Christiansen, 2004) of the resulting set of surface wave dispersion curves (Socco et al., 2009). Long and Kogaoglu (2001) proposed a tomographic approach based on surface wave group velocity.

All of these approaches, however, do not directly deal with the problem of a complex wave field where surface wave propagation is affected by the presence of sharp lateral heterogeneities. The presence of reflection/refraction phenomena induced by such heterogeneities has been recognized in large scale seismology and has led to the development of specific inversion procedures devoted to imaging bodies responsible for observed patterns in Rayleigh waves (e.g., Meier et al. 1997) and coda waves (e.g., Stich et al. 2009) registrations.

However, one should be aware that when we consider waves' scattering by the velocity heterogeneities, the concept of the velocity itself loses its meaning in the immediate neighborhood of the scatterers, since the generated (reflected, refracted, converted) waves are not yet spatially separated according to their types. This is the case for Rayleigh wave field sounding near the scattering heterogeneities (e.g., cavities) of wavelengths of the same or smaller size (Gorbatikov and

Tsukanov, 2011). Gorbatikov et al. (2008) suggested that, in this situation, monitoring lateral variations of ambient vibration average relative amplitudes can be considered as useful exploration tool to detect localized bodies. Numerical simulations and field experiences support this suggestion (Gorbatikov and Tsukanov, 2011).

In this context, an approach based on the concept of a “diffuse” wavefields can be considered more appropriate than a “classical” seismological approach based on the identification of seismic phases travelling in the medium to be explored. Recent theoretical studies have shown that the cross-correlation of diffuse wavefields can provide an estimate of the Green’s functions between receivers (Weaver & Lobkis 2001, 2004; Snieder, 2004; Wapenaar, 2004; Wapenaar & Fokkema, 2006). Using coda waves of seismic events (Campillo & Paul 2003) and long seismic noise sequences (Shapiro & Campillo 2004), it was confirmed that it is possible to estimate the Rayleigh wave component of Green’s functions between two stations by the cross-correlation of simultaneous recordings, a method now generally referred to as seismic interferometry. These results allowed the first attempts of surface wave tomography at regional scales (e.g. Shapiro & Campillo 2004; Sabra *et al.* 2005; Shapiro *et al.* 2005; Gerstoft *et al.* 2006; Yao *et al.* 2006; Cho *et al.* 2007; Lin *et al.* 2007; Yang *et al.* 2007) using seismic noise recordings from broad-band seismic networks. Generally, for these kinds of studies, waves at frequencies well below 1 Hz were used to image the crust and the upper-mantle structure. A comprehensive review of the seismic interferometry method can be found in Curtis *et al.* (2006).

Seismic noise interferometry can be also applied to frequencies greater than 1Hz. Schuster (2001) and Schuster *et al.* (2004) demonstrated the possibility of forming an image of the subsurface using the cross-correlation of seismic responses from natural and man-made sources at the surface or in the subsurface. Furthermore, within the context of exploration geophysics, Bakulin & Calvert (2004, 2006) first proposed a practical application of seismic interferometry, showing that it is possible in practice to create a virtual source at a subsurface receiver location in a well. Other recent applications for the high-frequency range have been proposed by Dong *et al.* (2006) and Halliday *et al.* (2007) for surface wave isolation and removal in active-source surveys. Among the several reasons that have stimulated the application of seismic noise interferometry to high frequencies, there is the possibility of applying this technique to suburban settings (Halliday *et al.* 2008), and then to exploit this approach for engineering seismology purposes. Such an application requires knowledge of the subsurface structure from depths of a few metres to several hundred metres, and for this reason interest has moved towards the high-frequency range. An application of seismic high frequency seismic interferometry to constrain damping profiles in the shallow subsoil was also provided by Albarello and Baliva (2009).

The application of seismic noise interferometry to high frequencies is not merely a change of scale, since it involves important questions still under discussion within the research community. For example, the effects of the high spatial and temporal variability in the distribution of noise sources occurring at high frequencies are still under investigation (Halliday & Curtis 2008a,b), as well as the relationship between the wavelength of interest and station interdistances. Several authors (e.g.. Chavez-Garcia & Luzon 2005; Chavez- Garcia & Rodriguez 2007; Yokoi & Margaryan 2008, ) showed, for a small scale experiment at a site with a homogeneous subsoil structure, the equivalence between the results obtained by crosscorrelation in the time domain and the SPAC method (Aki 1957). However, it is worth noting that for non-homogeneous subsoil conditions, SPAC suffers a severe drawback. That is, generally such a method is used to retrieve the shallow soil structure below a small array of sensors by means of the inversion of surface wave dispersion curves extracted by seismic noise analysis. In particular, the inversion is performed under the assumption that the structure below the site is nearly 1-D. Therefore, if the situation is more complicated (2-D or 3-D structure), then the SPAC method can only provide a biased estimate of the *S*-wave velocity structure. On the other hand, one can expect that, similarly to what is obtained over regional scales, local heterogeneities will affect the noise propagation between sensors, and hence can be retrieved

by analysing the Green's function estimated by the cross-correlation of the signals recorded at two different stations. For this reason, passive seismic interferometry is also believed to be a valuable tool for studying complex geological structure and estimating surface wave tomography for smaller spatial scales (Figure 24).

Recently, Picozzi et al. (2008) verified the suitability of seismic interferometry for seismic engineering and microzonation purposes. In fact, after having first evaluated the possibility of retrieving reliable and stable Green's functions within the limitations of time and instrumentation that bound standard engineering seismological experiments (for example, in urban microzonation studies, the number of deployed sensors is generally not larger than 20 and the acquisition time does not last more than a few hours) they applied the seismic interferometry technique to recordings from a 21-station array installed in the Nauen test site (Germany) ([http://www.geophysik.tuberlin.de/menue/testfeld\\_nauen/](http://www.geophysik.tuberlin.de/menue/testfeld_nauen/); Yaramanci *et al.* 2002). They showed that passive seismic interferometry is a valuable tool for the characterization of near-surface geology since the travel times estimated from the Green's functions analysis for different frequencies were inverted to derive, innovatively due to the frequency range investigated and the scale of the experiment, the laterally varying 3-D surface wave velocity structure below the array. Figure 25 shows the surface wave tomographic images for the frequencies 14 Hz and 6 Hz, as well as a 2D cross section of S-wave velocities highlighting the lateral velocity variations (Picozzi et al., 2008). Following Picozzi et al. (2008), Renalier et al. (2010) applied the same technique to data collected on a landslide.

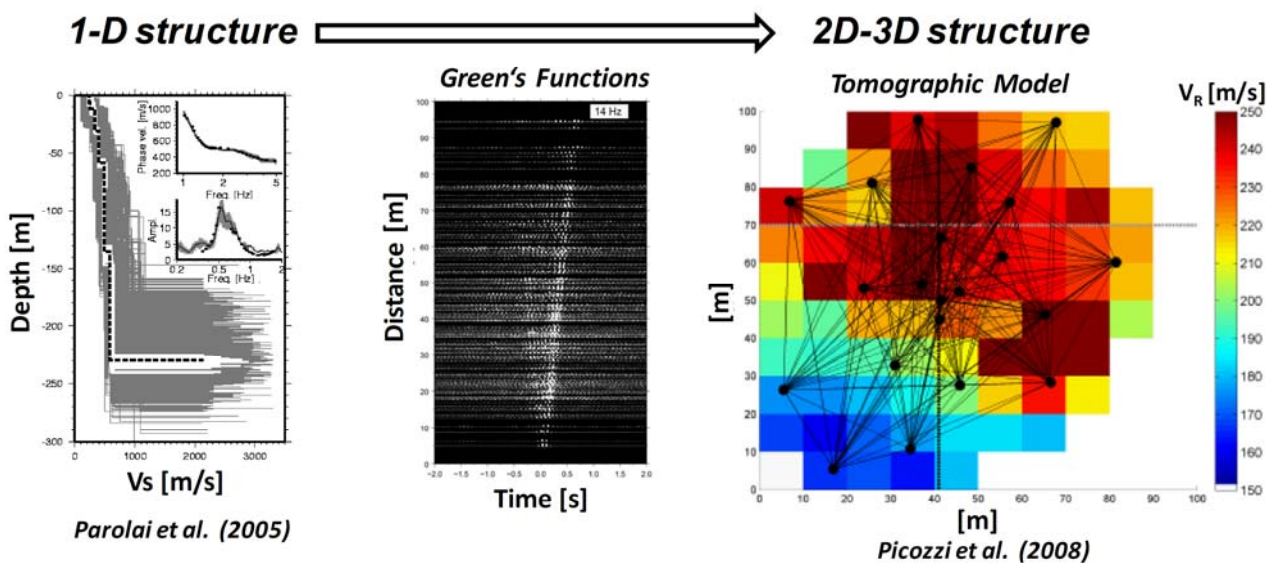


**Figure 24** – The perspective of surface wave investigations using seismic interferometry on sites with lateral velocity variations (modified from Parolai et al. 2005; and Picozzi et al., 2008).

## 8. Conclusions

Advantages of surface methods are mainly related to their non-invasive nature. They are more economical and can be performed more rapidly than borehole methods. Furthermore, in sites like solid waste disposals and landfills, due to environmental concerns, surface methods may be the only choice for geotechnical investigations. Another aspect of surface methods is related to the volume of soil involved in a survey, which is much larger than in borehole methods. As a result, surface methods are particularly useful if the average properties of a soil deposit are to be assessed, as in the case of ground response analyses.

A major limitation of surface wave methods is related to the model that is used for the interpretation. Typically a stack of linear elastic layers is used, hence surface wave tests cannot identify lateral variation and the final result is biased if the soil deposit does not resemble reasonably a simple layered medium. Several approaches proposed for the construction of 2D models from surface wave data are still based on a set of 1D inversions and as such they should be used with particular care and with a clear understanding of the actual procedure (Socco et al., 2009). However, the seismic interferometry approach of Picozzi et al. (2008) (see section 6) seems to be promising with respect of the capability of estimating 2 or 3D subsoil structure by surface wave analysis.

Because inverse problems are mathematically ill-posed, the non uniqueness of the solution plays a role. Indeed, several profiles which give numerical dispersion curves having a similar distance from the experimental dispersion curve can be identified. This problem is well known as equivalence in geophysical tests based on inverse problems. The implications are a certain degree of uncertainty in the final shear wave velocity profile. For example, surface wave tests are not the first choice as the objective is the exact location of an interface between different layers.

The resolution in the shear wave velocity profile that can be obtained with surface wave methods decreases with increasing depth. Thin layers are resolved if they are close to the surface, but they are not “seen” by the method if they are at depth.

Nonetheless, surface wave methods provide an excellent tool for soil characterization if the overall behaviour of the medium is to be identified. Their main advantage comes from the non-invasive nature of the test: all the measurements are performed from the ground surface with no need for boreholes. For this reason, they are more cost and time effective (e.g. no need for site preparation) and can be performed where it is not advisable to invade the medium (e.g. waste deposits).

Compared to seismic refraction using horizontally polarized shear waves, which is another way to obtain a shear wave velocity profile non-invasively, surface wave tests do not suffer limitations related to the actual site stratigraphy, being able to characterize the medium independently of the actual sequence of stiffer (faster) and softer (slower) layers. Indeed, refraction methods suffer in the presence of ‘hidden’ layers having certain ratios of thickness and/or velocity, which makes them not detectable.

The performances of surface wave tests are good even in noisy environments (e.g., urban areas or industrial sites). Other seismic tests based on the evaluation of first arrivals and travel time are much more difficult to interpret in the presence of background noise. The processing of surface wave data is done entirely in the frequency domain. The presence of excessive noise for specific frequencies does not compromise the possibility of interpreting the data. Background noise can even be used as a source of information using seismic noise surveys. In particular, this kind of analysis has the advantage of allowing investigations to very large depths (hundreds of meters to kilometres) that would be prohibitive with active source methods due to the lack of energy with standard sources in the low frequency range. Therefore, surface wave methods based on seismic noise analysis are particularly attractive for studying subsoil structure in urban areas and deep sedimentary basins.

The selection of appropriate technique (active, passive, active + passive) for a given site is related to the objective of the characterization: active methods are best suited for high resolution shallow characterization, whereas passive methods provide a greater penetration depth, but limited resolution close to the ground surface. In situations where both are necessary (deep characterization and high resolution at shallow depth), the combination of both active and passive data gives the optimal result (Richwalski et al., 2007; Foti et al., 2009).

Large volumes of soils are tested and the test results reflect the overall dynamic behaviour of the soil deposit. The degree of accuracy obtained by surface wave studies is typically in line with the assumptions and the simplifications adopted in the design stage. Moreover, the 1D model used for



the interpretation is also common for many engineering approaches for design and verification (as, for example, the code Shake for the evaluation of the seismic response of the site, see Foti et al., 2009). Despite this, the most important developments expected in the future involve the 1D approximation not needing to be adopted. This actually represents the more advanced input of current research, along with the development of suitable experimental configurations and processing tools for retrieving more parameters than S-waves profile (e.g., material damping, Poisson ratios, etc.) from surface wave measurements.

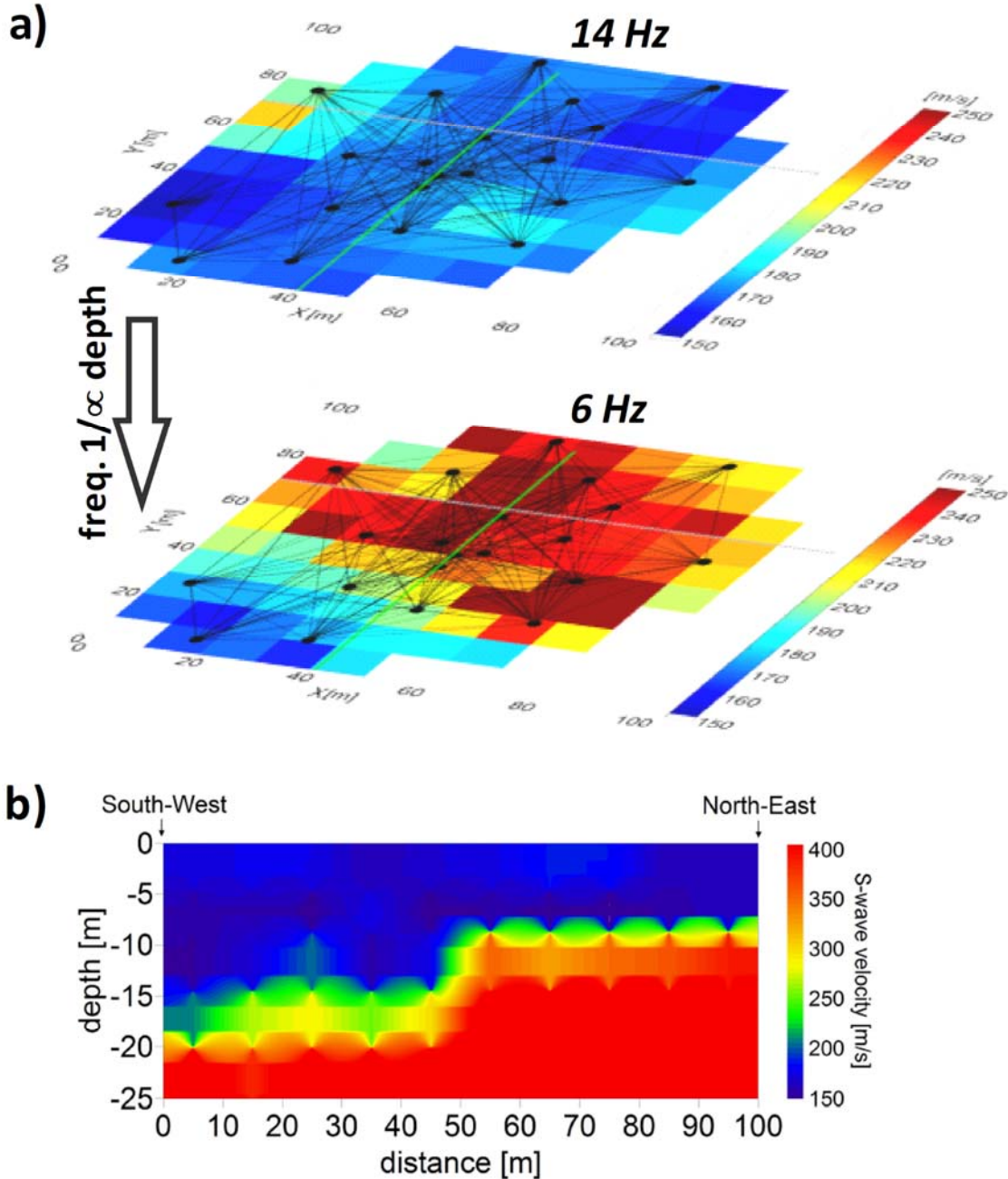


**Figure 25** – Tomographic inversion results from seismic noise interferometry analysis. *a)* Frequencies 14 Hz and 6 Hz. Locations of the DC geoelectric and GP radar profiles (green dotted line), and the field track (grey dotted line) are also shown. *b)* S-wave velocity section derived by seismic noise tomography extending southwest to northeast in the centre of the study area. (modified from Picozzi et al., 2008).

## ACKNOWLEDGEMENTS

This work has been developed as part of Project S4 of the Italian National Institute of Geophysics and Volcanology (INGV) funded by the Italian Civil Protection Department. Authors are grateful to two anonymous reviewers for their constructive comments. Figures 17 18 19 20 21 are reproduced with the kind permission of Springer ([License Number](#) 2657641495585, Apr 28, 2011). K Fleming kindly improved the English.

## REFERENCES

- Aki, K., 1957. Space and time spectra of stationary stochastic waves, with special reference to microtremors, *Bull. Earthq. Res. Inst.*, 35, 415-456.
- Aki, K., 1965, A note on the use of microseisms in determining the shallow structure of the Earth's crust: *Geophysics*, 30, 665-666
- Aki K., Richards P.G. 1980. Quantitative seismology: theory and methods - 2 vol. Freeman. S. Francisco
- Albarelo D. and Baliva F., 2009. In-situ estimates of material damping from environmental noise measurements. Mucciarelli, Marco; Herak, Marijan; Cassidy, John (Eds.), *Increasing Seismic Safety by Combining Engineering Technologies and Seismological Data (NATO Science for Peace and Security Series C: Environmental)*, Springer, XVIII, 382 pp., ISBN: 978-1-4020-9194-0, 73-84
- Albarelo D. and Lunedei E., 2010. Alternative interpretations of Horizontal to Vertical Spectral Ratios of ambient vibrations: new insights from theoretical modeling. *Bull. Earthq. Engng.*, 8, 3, 519-534, DOI: 10.1007/s10518-009-9110-0
- Arai, H., and K. Tokimatsu 2000. Effects of Rayleigh and Love waves on microtremor H/V spectra, paper presented at *12th World Conference on Earthquake Engineering*, N. Z. Soc. for Earthquake Eng., Auckland, N. Z.
- Arai, H., and K. Tokimatsu 2004. S-wave velocity profiling by inversion of microtremor H/V spectrum, *Bull. Seism. Soc. Am.* 94, 53–63.
- Arai, H. and K. Tokimatsu 2005. S-wave velocity profiling by joint inversion of microtremor dispersion curve and horizontal-to-vertical (H/V) spectrum. *Bull. Seism. Soc. Am.* 95, 1766-1778.
- Asten, MW (2006) On bias and noise in passive seismic data from finite circular array data processed using SPAC method. *Geophysics*, 71, V153-V162, doi:10.1190/1.2345054.
- Auken, E., and A. V. Christiansen, 2004, Layered and laterally constrained 2D inversion of resistivity data: *Geophysics*, 69, 752-761.
- Badsar, S. A., Schevenels, M., Haegeman, W., Degrande G. 2010. Determination of the material damping ratio in the soil from SASW tests using the half-power bandwidth method. *Geophysical Journal Int.*, 182 (3), 1493-1508
- Bakulin, A. & Calvert, R., 2004. Virtual source: new method for imaging and 4D below complex overburden, in *Proceedings of 74th Annual International Meeting (expanded abstracts)*, Society of Exploration Geophysicists, 2477–2480.
- Bakulin, A. & Calvert, R., 2006. The virtual source method: theory and case study, *Geophysics*, 71, S1139–S1150.
- Bard, P. Y. 1998 Microtremor measurement: a tool for site effect estimation? Second International Symposium on the Effects of the Surface Geology on Seismic Motion ESG98, Japan.

- Beaty, K. S., D. R. Schmitt, and M. Sacchi, 2002, Simulated annealing inversion of multimode Rayleigh wave dispersion curves for geological structure: *Geophysical Journal International*, 151, 622-631.
- Ben-Menahem A., Singh S.J., 2000. *Seismic waves and sources*, Dover Publications Inc., New York, 1102 pp.
- Birtill, J.W., and Whiteway, F.E., 1965. The application of phased arrays to the analysis of seismic body waves, *Philos. Trans. R. Soc. London*, Ser. A, 258, 421-493.
- Bohlen, T., S. Kugler, G. Klein, and F. Theilen, 2004, 1.5-D Inversion of lateral variation of Scholte wave dispersion: *Geophysics*, 69, 330-344
- Buchen, P.W. and Ben-Hador, R., 1996. Free-mode surface-wave computations, *Geophys. J. Int.*, **124**, 869–887.
- Campillo, M. and Paul, A., 2003. Long-range correlations in the seismic coda, *Science*, 299, 547–549.
- Capon, J., 1969. High-resolution frequency-wavenumber spectrum analysis, *Proc. IEEE*, 57, 8, 1408-1418.
- CEN, 2004. *EN 1998-1 Eurocode 8: Design of structures for earthquake resistance – Part 1: general rules, seismic actions and rules for buildings*. Brussels.
- Chavez-Garcia, F.J. & Luzon, F., 2005. On the correlation of seismic microtremors, *J. geophys. Res.*, 110, B11313, doi:10.1029/2005JB003671.
- Chavez-Garcia, F.J. & Rodriguez, M., 2007. The correlation of microtremors: empirical limits and relations between results in frequency and time domains, *Geophys. J. Int.*, 171, 657–664.
- Cho, K.H., Herrmann, R.B. & Ammon, C.J. & Lee, K., 2007. Imaging the upper crust of the Korean Peninsula by surface-wave tomography, *Bull. seism. Soc. Am.*, 97, 198–207, doi:10.1785/0120060096.
- Comina, C., Foti, S., Boiero, D., Socco, L.V. 2011. Reliability of  $V_{s,30}$  evaluation from surface waves tests, *Journal of Geotechn. and Geoenv. Eng.*, ASCE, 137(6), DOI: 10.1061/(ASCE)GT.1943-5606.0000452
- Curtis, A., Gerstoft, P., Sato, H., Snieder, R. & Wapenaar, K., 2006. Seismic interferometry—turning noise into signal, *Leading Edge*, 25, 1082–1092.
- D’Amico V., Picozzi M., Albarello D., Naso G. and Tropenscovino S., 2004. Quick estimate of soft sediments thickness from ambient noise horizontal to vertical spectral ratios: a case study in southern Italy”. *J. Earthq. Engineering*, 8, 6, 895-908
- D’Amico V., Picozzi M., Baliva F. and Albarello D., 2008. Ambient Noise Measurements for Preliminary Site-Effects Characterization in the Urban Area of Florence. *Bull. Seism. Soc. Am.*, 98, 3, 1373-1388, doi: 10.1785/0120070231
- Degrade, G., S. A. Badsar, G. Lombaert, M. Schevenels, and A. Teughels, 2008, Application of the coupled local minimizers method to the optimization problem in the spectral analysis of surface wave method: *Journal of Geotechnical and Geoenvironmental. Engineering*, 134, 10, 1541-1553.
- Delgado, J., C. Lopez Casado, A. C. Estevez, J. Giner, A. Cuenca and S. Molina 2000a. Mapping soft soils in the Segura river valley (SE Spain): a case study of microtremors as an exploration tool, *J. Appl. Geophys.* 45, 19–32.
- Delgado, J., C. Lopez Casado, J. Giner, A. Estevez, A. Cuenca, and S. Molina. 2000b. Microtremors as a geophysical exploration tool: applications and limitations, *Pure Appl. Geophys.* 157, 1445–1462. 1841.

- Dong, S., He, R. & Schuster, G., 2006. Interferometric prediction and leastsquares subtraction of surface waves, in *Proceedings of 76th Annual International Meeting* (expanded abstracts), Society of Exploration Geophysicists, 2783–2786.
- Douglas, A., 2002. Seismometer arrays – Their use in earthquake and test ban seismology, in *Handbook of Earthquake and Engineering Seismology*, edited by P. Jennings, H. Kanamori, and W. Lee, 357-367, Academic, San Diego, Calif.
- Dziewonski A.M., Bloch S. and Landisman M. 1969 A technique for the analysis of transient seismic signals. *Bull. Seism. Soc. Am.*, 59, 427-444
- Dziewonski A.M., Hales A.L. 1972. Numerical Analysis of Dispersed Seismic Waves. In *Methods in Computational Physics* vol.11 *Seismology: Surface waves and Earth Oscillations*. Bolt, B.A. Academic Press. New York: 39-85.
- Fäh, D., Kind, F., and Giardini, D., 2001, A theoretical investigation of average H/V ratios: *Geophys. J. Int.*, 145, 535-549.
- Fäh, D., Kind, F., and Giardini, D., 2003, Inversion of local S-wave velocity structures from average H/V ratios, and their use for the estimation of site-effects: *J. Seismology*, 7, 449-467.
- Field, E. H. and Jacob, K. 1993 "The theoretical response of sedimentary layers to ambient seismic noise", *Geophys. Res. Lett.* 20 24, 2925-2928.
- Foti S., 2000. Multistation Methods for Geotechnical Characterization using Surface Waves. PhD dissertation, Politecnico di Torino, Italy
- Foti S., 2003. Small Strain Stiffness and Damping Ratio of Pisa Clay from Surface Wave Tests. *Geotechnique*, 53(5): 455-461
- Foti S., 2004. Using Transfer Function for Estimating Dissipative Properties of Soils from Surface Wave Data. *Near Surface Geophysics*, EAGE, vol. 2 (4), 231-240
- Foti S. 2005. Surface Wave Testing for Geotechnical Characterization. in *Surface Waves in Geomechanics: Direct and Inverse Modelling for Soils and Rocks*, CISM Series, Number 481, Lai C.G. and Wilmanski K. eds, Springer, Wien, 47-71
- Foti S., Comina C., Boiero D., Socco L.V., 2009 "Non uniqueness in surface wave inversion and consequences on seismic site response analyses", *Soil Dynamics and Earthquake Engineering*, Vol. 29 (6), 982-993
- Foti S., Lancellotta R., Sambuelli L., Socco L.V., 2000 "Notes on fk analysis of surface waves", *Annali di Geofisica*, vol. 43, n.6, 1199-1210
- Foti S., Sambuelli L., Socco L.V., Strobbia C., 2003 Experiments of joint acquisition of seismic refraction and surface wave data, *Near Surface Geophysics*, EAGE, 119-129
- Frosch, R.A., and Green, P.E., 1966. The concept of the large aperture seismic array, *Proc. R. Soc. London*, Ser. A, 290, 368-384.
- Gabriels P., Snieder R., Nolet G., 1987. In situ measurements of shear-wave velocity in sediments with higher-mode Rayleigh waves. *Geophys. Prospect.* 35: 187-196
- Ganji V., Gukunski N., Nazarian S., 1998 "Automated inversion procedure for spectral analysis of surface waves", *J. Geotech. and Geoenv. Eng.*, vol. 124, ASCE, pp. 757-770
- García-Jerez, A., Luzón, F. and Navarro, M. (2008) An alternative method for calculation of Rayleigh and Love wave phase velocities by using three-component records on a single circular array without a central station. *Geophysical Journal International*, 173(3), 844-858 [doi: 10.1111/j.1365-246X.2008.03756.x](https://doi.org/10.1111/j.1365-246X.2008.03756.x).

- Gerstoft P., Sabra K.G., Roux P., Kuperman W.A. & Fehler M.C., 2006. Green's functions extraction and surface-wave tomography from microseisms in southern California, *Geophysics*, 71, 23–32.
- Goldberg D.E., 1989, Genetic algorithms in Search, Optimization and Machine Learning: Addison-Wesley.
- Gorbatikov, A.V., Stepanova M.Yu., and Korablev, G.E., 2008. Microseismic Field Affected by Local Geological Heterogeneities and Microseismic Sounding of the Medium, *Fiz. Zemli*, no. 7, pp. 66–84 [*Izv. Phys. Earth* (Engl. Transl.), 2008, vol. 44, no. 7, pp. 577–592].
- Gorbatikov, A. V.; Tsukanov, A. A., 2011: Simulation of the Rayleigh wave in the proximity of the scattering velocity heterogeneities. Exploring the capabilities of the microseismic sounding method, *Izvestiya Physics of the Solid Earth* 47, 4, 354-369
- Grandjean, G., and A. Bitri, 2006, 2M-SASW: Multifold multichannel seismic inversion of local dispersion of Rayleigh waves in laterally heterogeneous subsurfaces: application to the Super-Sauze earthflow, France: *Near Surface Geophysics*, 4, 367-375.
- Halliday D.F. & Curtis A., 2008a. Seismic interferometry, surface waves, and source distribution, *Geophys. J. Int.*, doi:10.1111/j.1365-246X.2008.03918.x.
- Halliday D.F. & Curtis A., 2008b. Seismic interferometry of scattered surface waves in attenuative media, submitted.
- Halliday D.F., Curtis A., Robertsson J.O.A. & van Manen D.-J., 2007. Interferometric surface-wave isolation and removal, *Geophysics*, 72, A67–A73.
- Halliday D.F., Curtis A. & Kragh E., 2008. Seismic surface waves in a suburban environment—active and passive interferometric methods, *Leading Edge*, 27, 210–218.
- Haney, M. M., Decker K. T., and Bradford J. H., 2010, Permittivity Structure Derived from Group Velocities of Guided GPR Pulses: in Miller, R. D., Bradford, J. H., Holliger, K., eds., *Advances in Near Surface Seismology and Ground-Penetrating Radar*, Society of Exploration Geophysicists, Tulsa, OK, 167-184
- Harkrider D.G., 1964. Surface waves in multi-layered elastic media. I Rayleigh and Love waves from buried sources in a multilayered elastic half space. *Bull. Seism. Soc. Am.* 54, 627–679.
- Herrmann, R.B., 1987. *Computer Programs in Seismology*, Vol. IV, St. Louis University, MO, USA.
- Hisada Y., 1994. An efficient method for computing Green's functions for a layered halfspace with sources and receivers at close depths. *Bull. Seism. Soc. Am.* 84, 1456–1472.
- Hobiger, M., P.-Y. Bard, C. Cornou, N. Le Bihan, 2009. Single Station Determination of Rayleigh Wave Ellipticity by Using the Random Decrement Technique (RayDec), *Geophys. Res. Lett.*, 36, 14, doi:10.1029/2009GL038863, 2009.
- Horike, M., 1985. Inversion of phase velocity of long period micro tremors to the S-wave velocity structure down to the basement in urbanized areas, *J. Phys. Earth*, 33, 59-96.
- Hough S.E., Seeber L., Rovelli A., Malagnini L., DeCesare A., Selvaggi G., and Lerner-Lam A., 1992. Ambient noise and weak motion excitation of sediment resonances: results from the Tiber Valley, Italy, *Bull. Seism. Soc. Am.*, 82, 1186-1205.
- Ivanov, J., R.D. Miller, J. Xia, D. Steeples, and C.B. Park, 2006, Joint analysis of refractions with surface waves: an inverse solution to the refraction-traveltime problem. *Geophysics*, 71, 6, R131–R138

- Jones R.B., 1958. In-situ measurement of the dynamic properties of soil by vibration methods. *Geotechnique*, 8 (1), 1-21
- Káráson, H., and van der Hilst, R.D., 2001. Tomographic imaging of the lowermost mantle with differential times of refracted and diffracted core phases (PKP, Pdiff), *J. Geophys. Res.*, 106, 6569-6587
- Karray, M. and Lefebvre, G., 2000. Identification and isolation of multiple modes in Rayleigh wave testing methods. *ASCE Proceedings Use of Geophysical Methods in Construction*, Geo Denver, pp. 80–94.
- Kind, F., Fäh, D., Giardini, D., 2005. Array measurements of S-wave velocities from ambient vibrations, *Geophysical Journal International*, 160, 114-126.
- Krüger, F., Baumann, M., Scherbaum, F., and Weber, M., 2001. Mid mantle scatterers near the Mariana slab detected with a double array method, *Geophys. Res. Lett.*, 28, 667-670.
- Kværna, T., 1989. On exploitation of small-aperture NORESS type arrays for enhanced Pwave detectability, *Bull. Seismol. Soc. Am.*, 79, 888-900.
- Ibs-von Seht, M., and J. Wohlenberg, 1999. Microtremor measurements used to map thickness of soft sediments, *Bull. Seism. Soc. Am.* 89, 250–259.
- Lacoss, R.T., Kelly, E.J., Toksöz, M.N., 1969. Estimation of seismic noise structure using arrays, *Geophysics*, 34, 21-38.
- Lai C.G. and Wilmanski K. (eds), 2005. Surface waves in geomechanics: direct and inverse modelling for soils and rocks, Springer, Wien, pp. 385
- Lai C.G., 1998. Simultaneous inversion of Rayleigh phase velocity and attenuation for near-surface site characterization. PhD Diss., Georgia Inst. of Techn., Atlanta (Georgia, USA)
- Lai C.G. and Rix G.J., 2002. Solution of the Rayleigh eigenproblem in viscoelastic media. *Bull. Seism.Soc. Am.*, 92(6), 2297–2309
- Lai C.G., Rix G.J., Foti S., Roma V., 2002. Simultaneous Measurement and Inversion of Surface Wave Dispersion and Attenuation Curves. *Soil Dynamics and Earthquake Engineering*, 22 (9-12), 923-930
- Lermo, J. and Chavez-Garcia, F. J., 1993. Site effect evaluation using spectral ratios with only one station. *Bull. Seism. Soc. Am.* 85, 5, 1574-1594.
- Lermo, J. and Chavez-Garcia, F. J., 1994. Are microtremors useful in site response evaluation? *Bull. Seism. Soc. Am.* 84, 135, 1364.
- Levshin A., Ratnikova L. and Berger J., 1992, Peculiarities of surface-wave propagation across central Eurasia. *Bull. Seism. Soc. Am.* 82, 2464-2493
- Lin, F.-C., Ritwoller, M.H., Townend, J., Bannister, S. & Savage M.K., 2007. Ambient noise Rayleigh wave tomography of New Zealand, *Geophys. J. Int.*, 170, 649–666, doi:10.1111/j.1365–246X.2007.03414x.
- Long, L.T., & Kocaoglu, A.H., 2001. Surface-Wave Group-Velocity Tomography for Shallow Structures. *Journal of Environmental and Engineering Geophysics Publications*, 71-81.
- Louie J.N., 2001. Faster, better: shear-wave velocity to 100 meters depth from refraction
- Lunedei E. and Albarello D., 2009. On the seismic noise wave field in a weakly dissipative layered Earth. *Geophys.J.Int.*, DOI: 10.1111/j.1365-246X.2008.04062.x

- Lunedei E., Albarello D., 2010. Theoretical HVSR from the full wave field modelling of ambient vibrations in a weakly dissipative layered Earth. *Geophys.J.Int.* 181, 1093-1108, doi: 10.1111/j.1365-246X.2010.04560.x
- Malagnini, L., Rovelli, A., Hough, S.E., and Seeber, L., 1993, Site amplification estimates in the Garigliano Valley, Central Italy, based on dense array measurements of ambient noise: *Bull. Seism. Soc. Am.*, 83, 1744-1755.
- Malagnini L., Herrmann R.B., Biella G., de Frando R., 1995. Rayleigh waves in quaternary alluvium from explosive sources: determination of shear-wave velocity and Q structure. *Bull. of Seism. Soc. of A.*, 85, pp. 900-922.
- Malagnini, L., Hermann, R.B., Mercuri, A., Opice, S., Biella, G. & De Franco, R., 1997. Shear-wave velocity structure of sediments from the inversion of explosion-induced Rayleigh waves: comparison with crosshole measurements, *Bull. seism. Soc. Am.*, 87, 1413–1421.
- Malischewsky P. G., Scherbaum F. 2004. Love's formula and H/V-ratio (ellipticity) of Rayleigh waves. *Wave Motion*, 40, 57–67
- Maraschini M., Ernst F., Foti S., Socco V., 2010. A new misfit function for multimodal inversion of surface waves. *Geophysics*, 75 (4), 31-43
- Maraschini M., Foti S. 2010. A Monte Carlo multimodal inversion of surface waves. *Geophysical Journal Int.*, 182 (3), 1557-1566
- McMechan G.A., Yedlin M.J., 1981. Analysis of dispersive waves by wave field transformation. *Geophysics*. 46: 869-874
- Menke, W., 1989, *Geophysical data analysis: discrete inverse theory*. rev. ed. Academic, San Diego, Calif.
- Meier, T., Malischewsky, P. G., Neunhoefer, H., 1997. Reflection and transmission of surface waves at a vertical discontinuity and imaging of lateral heterogeneity using reflected fundamental Rayleigh waves, *Bull. of the Seismol. Soc. Am.* 87, 6, 1648-1661
- Mosegaard, K., and M. Sambridge, 2002, Monte Carlo analysis of inverse problems, *Inverse Problems*, **18**, R29-R54.
- Moss, R.E.S. 2008. Quantifying measurement uncertainty of thirty-meter shear-wave velocity. *Bull. Seism. Soc. Am.*, 98 (3), 1399 – 1411.
- Mucciarelli, M., 1998 Reliability and applicability of Nakamura's technique using microtremors: an experimental approach, *J. Earthq. Engrg.* 2, 625 638.
- Mulargia F. and Castellaro S., 2008. Passive Imaging in Nondiffuse AcousticWavefields. *Phys.Rev.Lett.*, 100, 218501
- Nakamura, Y., 1989, A method for dynamic characteristics estimations of subsurface using microtremors on the ground surface: *Q. Rept. RTRI Jpn.*, 30, 25-33.
- Nazarian S., Stokoe II K.H., 1984. In situ shear wave velocities from spectral analysis of surface waves. *Proc. 8th Conf. on Earthquake Eng. - S.Francisco*, vol. 3, Prentice-Hall, pp. 31-38
- Nazarian S., Desai M.R., 1993 Automated surface wave method: field testing. *J. Geotechnical Eng.*, vol. 119 (7), ASCE, pp. 1094-1111
- Neducza, B., 2007, Stacking of surface waves: *Geophysics*, 72, 2, V51-V58.
- Nelder, J.A., and Mead, R., 1965, A simplex method for function minimization: *Comp. J.*, 7, 308-313.



- NEHRP (2000). NEHRP Recommended provisions for seismic regulations for new buildings and other structures, Part 1,: Provisions, FEMA 368. Washington, DC: Federal Emergency Management Agency.
- Nogoshi, M., and T. Igarashi, 1970. On the propagation characteristics of microtremors, *J. Seism. Soc. Japan* 23, 264–280 (in Japanese with English abstract).
- Nogoshi, M. and Igarashi, T., 1971. On the amplitude characteristics of microtremor (Part 2). *J. Seism. Soc. Japan* 24, 26–40.
- Okada, H., 2003. The Microtremor Survey Method. Geophys, Monograph Series, SEG, 129 pp.
- Ohori, M., Nobata, A., and Wakamatsu, K., 2002. A comparison of ESAC and FK methods of estimating phase velocity using arbitrarily shaped microtremor analysis, *Bull. Seism. Soc. Am.*, 92, 2323–2332.
- Ohrnberger, M.; Vollmer, D.; Scherbaum, F. WARAN-a mobile wireless array analysis system for in-field ambient vibration dispersion curve estimation. In Proceedings of the 1<sup>st</sup> ECEES. Geneva, Switzerland. 3–8 September 2006, p284.
- O'Neill A., 2004. Full waveform reflectivity for inversion of surface wave dispersion in shallow site investigations, *Proc. ISC-2 on Geotechnical and Geophysical Site Characterization*, Viana da Fonseca & Mayne (eds.), Millpress, Rotterdam, 547–554
- Park C.B., Miller R.D., Xia J., 1999. Multichannel analysis of surface waves. *Geophysics* 64: 800–808
- Parolai S, Bormann P, Milkereit C., 2001. Assessment of the natural frequency of the sedimentary cover in the Cologne area (Germany) using noise measurements. *J. Earthq. Engrg.* 5, 541–564.
- Parolai, S., Picozzi, M., Richwalski, S.M., and Milkereit C., 2005. Joint inversion of phase velocity dispersion and H/V ratio curves from seismic noise recordings using a genetic algorithm, considering higher modes, *Geoph. Res. Lett.*, 32, doi: 10.1029/2004GL021115.
- Parolai, S., Richwalski, S.M., Milkereit, C. & Faeh, D., 2006. S-wave velocity profile for earthquake engineering purposes for the Cologne area (Germany), *Bull. Earthq. Eng.*, 65–94, doi:10.1007/s10518-005-5758-2.
- Parolai, S., Mucciarelli, M., Gallipoli, M.R., Richwalski, S.M., and Strollo, S., 2007. Comparison of Empirical and Numerical Site Responses at the Tito Test Site, Southern Italy, *Bull. Seism. Soc. Am.*, 97, 1413–1431.
- Pedersen H.A., Mars J.I., Amblard P., 2003. Improving surface-wave group velocity measurements by Energy reassignment. *Geophysics*, 68, 677–684
- Picozzi, M. & Albarello, D., 2007. Combining genetic and linearized algorithms for a two-step joint inversion of Rayleigh wave dispersion and H/V spectral ratio curves. *Geophys. J. Int.*, 169, 189–200.
- Picozzi, M., S. Parolai and D. Albarello, 2005a. Statistical analysis of noise horizontal to-vertical spectral ratios (HVSr), *Bull. Seism. Soc. Am.*, 95, 1779–1786.
- Picozzi, M., Parolai, S., Richwalski, S.M. (2005b) Joint inversion of H/V ratios and dispersion curves from seismic noise: Estimating the S-wave velocity of bedrock. *Geoph. Res. Lett.*, 32, No.11 doi: 10.1029/2005GL022878.
- Picozzi, M.; Parolai, S.; Bindi, D.; Strollo, A., 2008: Characterization of shallow geology by high-frequency seismic noise tomography, *Geophysical Journal International*, 176, 1, 164–174.



- Picozzi, M., Strollo, A., Parolai, S., Durukal, E., Özel, O., Karabulut, S., Zschau, J., and M. Erdik, M. (2008). Site characterization by seismic noise in Istanbul, Turkey. *Soil Dynamic and Earthquake Engineering*, 29 (2009) 469– 482, doi:10.1016/j.soildyn.2008.05.007.
- Picozzi, M.; Milkereit, C.; Parolai, S.; Jaeckel, K.-H.; Veit, I.; Fischer, J.; Zschau, J. GFZ Wireless Seismic Array (GFZ-WISE), a Wireless Mesh Network of Seismic Sensors: New Perspectives for Seismic Noise Array Investigations and Site Monitoring. *Sensors* 2010a, 10, 3280-3304.
- Picozzi, M., Parolai, S., and Bindi, D. (2010b). De-blurring of frequency-wavenumber images from small-size seismic arrays. *Geophysical Journal International*, 181, 1, 357-368. DOI: 10.1111/j.1365-246X.2009.04471.x
- Poggiagliolmi E., Berkhout A.J., Boone M.M., 1982 “Phase unwrapping, possibilities and limitations”, *Geophysical Prospecting*, vol. 30, pp. 281-291
- Press, F., 1968. Earth models obtained by Monte Carlo inversion. *Journal of Geophysical Research* 73, 5223-5234.
- Press, W.H., Teukolsky, S.A., Vetterling, W.T., and Flannery, B.P., 1986, *Numerical Recipes in Fortran 77, The Art of Scientific Computing*: Cambridge University Press.
- Renalier, F., D. Jongmans, M. Campillo, and P. Y. Bard. 2010. Shear wave velocity imaging of the Avignonet landslide (France) using ambient noise cross correlation, *J. Geophys. Res.*, 115, F03032, doi:10.1029/2009JF001538.
- Richwalski, S.; Picozzi, M.; Parolai, S.; Milkereit, C.; Baliva, F.; Albarello, D.; Row-Chowdhury, K.; van der Meer, H.; Zschau, J., 2007: Rayleigh wave dispersion curves from seismological and engineering-geotechnical methods: a comparison at the Bornheim test site (Germany), *Journal of Geophysics and Engineering*, 4, 349-361.
- Ritter, J.R.R., Jordan, M., Christensen, U., and Achauer, U., 2001. A mantle plume below the Eifel volcanic fields, Germany, *Earth Planet. Sci. Lett.*, 186, 7-14.
- Rix, G.J., Lai, C.G., Spang, A.W. 2000. In Situ Measurements of Damping Ratio Using Surface Waves. *Journal of Geotechnical and Geoenvironmental Engineering* 126, ASCE, 472-480
- Roesset J.M., Chang D.W., Stokoe K.H., 1991 “Comparison of 2-D and 3-D models for analysis of surface wave tests”, *Proc. 5th Int. Conf. on Soil Dyn. and Earthq. Eng.*, Karlsruhe, vol. 1, pp. 111-126
- Rost, S., and Thomas, C., 2002. Array Seismology: Methods and Applications, *Reviews of Geophysics*, 40, 3.
- Sabra, K.G., Gerstoft, P., Roux, P., Kuperman, W.A. & Fehler, M.C., 2005. Surfacewave tomography from microseisms in Southern California, *Geophys. Res. Lett.*, 32, L14311, doi:10.1029/2005GL023155.
- Sambridge, M., 1999a, Geophysical inversion with a Neighbourhood algorithm-I. Searching parameter space: *Geophysical Journal International.*, 138, 479-494.
- Sambridge, M., 1999b, Geophysical Inversion with a Neighbourhood Algorithm - II. Appraising the ensemble: *Geophysical Journal International*, 138, 727-746.
- Santamarina J.C., Fratta D., 1998. Introduction to discrete signals and inverse problems in civil engineering. Asce Press. Reston
- Scherbaum, F., Hinzen, K.-G., and Ohrnberger, M., 2003. Determination of shallow shearwave velocity profiles in Cologne, Germany area using ambient vibrations, *Geophys. J. Int.*, 152, 597-612.

- Schnabel, P. B., Lysmer, J., and Seed, H. B. 1972. SHAKE: A computer program for earthquake response analysis of horizontally layered sites. Rep. No. EERC/72-12, Earthquake Engineering Research Center, Univ. of California, Berkeley, Calif.
- Schuster, G.T., 2001. Theory of daylight/interferometric imaging: tutorial, in *Proceedings of 63rd Meeting, European Association of Geoscientists and Engineers*, Session: A32 (extended Abstracts).
- Schuster, G.T., Yu, J., Sheng, J. & Rickett, J., 2004. Interferometric/daylight seismic imaging, *Geophys. J. Int.*, 157, 838–852.
- SESAME, 2003. Final report on measurements guidelines, LGIT Grenoble, CETE Nice, WP02, H/V technique: experimental conditions, [http://sesame-fp5.obs.ujf-grenoble.fr/Delivrables/D08-02\\_Texte.pdf](http://sesame-fp5.obs.ujf-grenoble.fr/Delivrables/D08-02_Texte.pdf)
- Shapiro, N.M. & Campillo, M., 2004. Emergence of broadband Rayleigh waves from correlations of the ambient seismic noise, *Geophys. Res. Lett.*, 31, L07614, doi:10.1029/2004GL019491.
- Shapiro, N.M., Campillo, M., Stehly, L. & Ritzwoller, M., 2005. High resolution surface wave tomography from ambient seismic noise, *Science*, 307, 1615–1618.
- Snieder, R., Scattering of surface waves , in *Scattering and Inverse Scattering in Pure and Applied Science*, Eds. Pike, R. and P. Sabatier, Academic Press, San Diego, 562-577, 2002
- Snieder, R., 2004. Extracting the Green's function from the correlation of coda waves: a derivation based on stationary phase, *Phys. Rev. E*, 69, doi:10.1103/PhysRevE.69.046610.
- Socco, L.V. and Strobbia, C., 2004 Surface Wave Methods for near-surface characterisation: a tutorial. *Near Surface Geophysics* 2(4), 165-185.
- Socco L.V., Boiero D., 2008. “Improved Monte Carlo inversion of surface wave data”, *Geophysical Prospecting*, Volume 56 Issue 3, Pages 357 – 371.
- Socco L.V., Boiero D. , Foti S., Piatti C. 2010a. Chapter 4: Advances in surface wave and body wave integration: in Miller, R. D., Bradford, J. H., Holliger, K., eds., *Advances in Near Surface Seismology and Ground-Penetrating Radar*, Society of Exploration Geophysicists, Tulsa, OK, 37-54
- Socco L.V., Boiero D., Foti S., Wisén R., 2009. “Laterally constrained inversion of ground roll from seismic reflection records”, *Geophysics*, SEG, in press
- Socco L.V., Foti S., Boiero D. 2010b. Surface wave analysis for building near surface velocity models: established approaches and new perspectives. *Geophysics*, SEG, 75, A83-A102
- Stephenson, W.J., Louie, J.N., Pullammanappallil, S., Williams, R.A., and Odum, J.K., 2005. Blind Shear-wave velocity comparison of ReMi and MASW results with boreholes to 200 m in Santa Clara Valley: implication for earthquake ground motion assessment. *Bull. Seism. Soc. Am.*, 95, 2506-2516.
- Stich, D., Danecek, P., Morelli, A., Tromp, J., 2009. Imaging lateral heterogeneity in the northern Apennines from time reversal of reflected surface waves, *Geophys. J. Int.*, 177, 543-554.
- Stokoe K.H. II, Wright S.G., J.A. Bay, J.M. Roesset., 1994. Characterization of geotechnical sites by SASW method. *Geophysical Characterization of Sites*. R.D. Woods Ed.: 15-25.
- Strobbia C., and Cassiani G., 2007. Multilayer ground-penetrating radar guided waves in shallow soil layers for estimating soil water content. *Geophysics*, 72(4), J17-J29.
- Strobbia, C., and S., Foti, 2006, Multi-Offset Phase Analysis of Surface Wave Data (MOPA): *Journal of Applied Geophysics*, 59, 300-313.

- Strollo, A.; Parolai, S.; Jäkel, K.-H.; Marzorati, S.; Bindi, D. 2008. Suitability of Short-Period Sensors for Retrieving Reliable H/V Peaks for Frequencies Less Than 1 Hz, *Bull. Seism. Soc. Am.*, 98, 2, 671-681.
- Szelwis R., Behle A., 1987. Shallow shear-wave velocity estimation from multimodal Rayleigh waves, in Danbom, S. and Domenico, S. N., Ed., *Shear-wave exploration: Soc. Expl. Geophys.*, pp.214-226.
- Tada, T., Cho I., Shinozaki Y. (2006). Atwo- radius circular array method: inferring phase velocity of Love waves using microtremor records. *Geophys res. Lett* 33, L10303.doi:10.1029/2006GL025722.
- Tanimoto T. and Alvizuri C., 2006. Inversion of the HZ ratio of microsisms fopr S-wave velocity in the crust. *Geophys.J.Int.*, 165, 323-335
- Tarantola A., 2005 *Inverse problem theory and methods for model parameter estimation*. Siam, Philadelphia, 1-55.
- Thorson, J. R., and J. F. Claerbout, 1985. Velocity-stack and slant-stack stochastic inversion, *Geophysics* 50, 2727–2741.
- Tian, G., D. W. Steeples, J. Xia, and K. T. Spikes, 2003, Useful resorting in surface-wave method with the Autojuggie: *Geophysics*, 68, 1906-1908
- Tokimatsu, K., Kuwayama, S., Tamura, S., and Miyadera, Y., 1991, Vs determination from steady state Rayleigh wave method: *Soils and Foundations*, 31, 153-163.
- Tokimatsu, K., S. Tamura, and H. Kojima, 1992. Effects of multiple modes on Rayleigh wave dispersion characteristics. *Journal of Geotechnical Engineering* 118, 1529–1543.
- Tokimatsu K., 1995 *Geotechnical Site Characterisation using Surface Waves*. Proc. IS Tokyo 1995, Balkema, 1333-1368
- Tuan T.T., Scherbaum F., Malischewsky P.G., 2011. On the relationship of peaks and troughs of the ellipticity (H/V) of Rayleigh waves and the transmission response of single layer over half-space models. *Geophys.J.Int.*, 184, 793-800
- Tselentis G-A., Delis G, 1998. Rapid assessment of S-wave profiles from the inversion of multichannel surface wave dispersion data. *Annali di Geofisica*. 41. 1-15
- van der Kruk, J. R., Jacob W., and Vereecken H. 2010, Properties of precipitation-induced multilayer surface waveguides derived from inversion of dispersive TE and TM GPR data, *Geophysics*, 75(4), WA263.
- Van der Sluis, A., and Van der Vorst, H.A., 1987, Numerical solution of large sparse linear algebraic system arising from tomographic problems, *in Seismic Tomography*, edited by G. Nolet: D. Reidel, pp. 49-83, Norwell, Mass.
- Wapenaar, K., 2004. Retrieving the elastodynamic Green's function of an arbitrary inhomogeneous medium by cross correlation, *Phys. Rev. Lett.*, 93, 25 4301–1-4.
- Wapenaar, K. & Fokkema, J., 2006. Green's function representations for seismic interferometry, *Geophysics*, 71, SI33–SI44.
- Wathelet, M., D. Jongmans, and M. Ohrnberger, 2004, Surface-wave inversion using a direct search algorithm and its application to ambient vibration measurements: *Near Surface Geophysics*, 2, 211-221.
- Weaver, R.L. & Lobkis, O.I., 2001. Ultrasonics without a source: thermal fluctuation correlation at MHz frequencies, *Phys. Rev. Lett.*, 87, 134301–134304.

- Weaver, R.L. & Lobkis, O.I., 2004. Diffuse fields in open systems and the emergence of the Green's function, *J. acoust. Soc. Am.*, 116, 2731–2734.
- Whiteway, F.E., 1966. The use of arrays for earthquake seismology, *Proc. R. Soc. London, Ser. A*, 290, 328–348.
- Xia, J., Miller, R.D., Park, C.B., Tian, G. 2002. Determining Q of near-surface materials from Rayleigh waves. *Journal of Applied Geophysics*, 51, 121–129
- Yang, Y., Ritzwoller, M.H., Levshin, A.L. & Shapiro, N.M., 2007. Ambient noise Rayleigh wave tomography across Europe, *Geophys. J. Int.*, 168, 259–274, doi:10.1111/j.1365-246X.2006.03203.x
- Yamanaka, H., M. Takemura, H. Ishida, and M. Niwa, 1994. Characteristics of long-period microtremors and their applicability in the exploration of deep sedimentary layers, *Bull. Seism. Soc. Am.* 84, 1831–1841.
- Yamanaka, H., and Ishida, H., 1996. Application of Generic algorithms to an inversion of surface-wave dispersion data. *Bull. Seism. Soc. Am.* 86, 436–444.
- Yao, H., Van Der Hilst, R.D. & De Hoop, M.V., 2006. Surface-wave array tomography in SE Tibet from ambient seismic noise and two station analysis: I—phase velocity maps, *Geophys. J. Int.*, 166, 732–744.
- Yaramanci, U., Lange, G. & Hertrich, M., 2002. Aquifer characterisation using Surface NMR jointly with other geophysical techniques at the Nauen/Berlin test site, *J. Appl. Geophys.*, 50, 47–65.
- Yokoi, T. & Margaryan, S., 2008. Consistency of the spatial autocorrelation method with seismic interferometry and its consequence, *Geophys. Prosp.*, 56, 435–451.
- Zhang, S.X. and L.S. Chan, 2003. Possible effects of misidentified mode number on Rayleigh wave inversion. *Journal of Applied Geophysics* 53, 17–29.
- Zhang, S.H., Chan, L.S. and Xia, J., 2004. The selection of field acquisition parameters for dispersion images from multichannel surface wave data. *Pure and Applied Geophysics* 161, 185–201.
- Zywicki, D.J., 1999. Advanced Signal Processing Methods Applied to Engineering Analysis of Seismic Surface Waves. PhD thesis at Georgia Institute of Technology